

1 **Perceptual saccadic suppression starts in the retina**

2 Saad Idrees<sup>1†</sup>, Matthias P. Baumann<sup>1,2†</sup>, Felix Franke<sup>3</sup>, Thomas A. Münch<sup>1,4\*</sup>, Ziad  
3 M. Hafed<sup>1,2\*</sup>

4  
5 <sup>1</sup>Werner Reichardt Centre for Integrative Neuroscience, Tübingen University, Tübingen, Germany  
6 72076

7 <sup>2</sup>Hertie Institute for Clinical Brain Research, Tübingen University, Tübingen, Germany 72076

8 <sup>3</sup>Bio Engineering Laboratory, ETH Zürich, Basel, Switzerland 4058

9 <sup>4</sup>Institute for Ophthalmic Research, Tübingen University, Tübingen, Germany 72076

10

11 \*Correspondence to:

12 [ziad.m.hafed@cin.uni-tuebingen.de](mailto:ziad.m.hafed@cin.uni-tuebingen.de) and [thomas.muench@uni-tuebingen.de](mailto:thomas.muench@uni-tuebingen.de)

13

14 †Equal contributions

15 \*Co-corresponding authors

16

17 **Corresponding author addresses:**

18 Ziad M. Hafed

19 Werner Reichardt Centre for Integrative Neuroscience

20 and

21 Hertie Institute for Clinical Brain Research

22 Otfried-Mueller Str. 25

23 Tuebingen, 72076

24 Germany

25 Phone: +49 7071 29 88819

26

27 and

28 Thomas A. Münch

29 Institute for Ophthalmic Research

30 and

31 Werner Reichardt Centre for Integrative Neuroscience

32 Otfried-Mueller Str. 25

33 Tuebingen, 72076

34 Germany

35 **Abstract**

36 Visual sensitivity, probed through perceptual detectability of very brief visual stimuli,  
37 is strongly impaired around the time of rapid eye movements. This robust perceptual  
38 phenomenon, called saccadic suppression, is frequently attributed to active  
39 suppressive signals that are directly derived from eye movement commands. Here  
40 we show instead that visual-only mechanisms, activated by saccade-induced image  
41 shifts, can account for all perceptual properties of saccadic suppression that we have  
42 investigated. Such mechanisms start at, but are not necessarily exclusive to, the very  
43 first stage of visual processing in the brain, the retina. Critically, neural suppression  
44 originating in the retina outlasts perceptual suppression around the time of saccades,  
45 suggesting that extra-retinal movement-related signals, rather than causing  
46 suppression, may instead act to shorten it. Our results demonstrate a far-reaching  
47 contribution of visual processing mechanisms to perceptual saccadic suppression,  
48 starting in the retina, without the need to invoke explicit motor-based suppression  
49 commands.

## 50 **Introduction**

51 Saccadic eye movements are a prominent feature of visual behavior; they allow  
52 successive sampling of visual information from the environment. However, from the  
53 perspective of the flow of visual information into the brain, these rapid eye  
54 movements constitute highly disruptive visual events, introducing spurious motions  
55 that should normally go unnoticed, or get canceled, at the level of perception. The  
56 question of how and why such perceptual cancellation takes place across saccades  
57 has intrigued philosophers and scientists for many decades<sup>1-4</sup>. Indeed, visual  
58 sensitivity to brief visual probes is strongly impaired around the time of saccades, in a  
59 phenomenon known as saccadic suppression that has repeatedly been  
60 demonstrated in a multitude of experiments<sup>5-15</sup>.

61  
62 Despite the robustness of saccadic suppression as a perceptual phenomenon, the  
63 mechanisms behind it remain highly controversial. On the one hand, perceptual  
64 saccadic suppression may arise through internal knowledge of planned eye  
65 movements and their associated motor commands<sup>5,13,16-19</sup>. According to this popular  
66 view, internal knowledge of eye movement commands is a necessary prerequisite for  
67 saccadic suppression: a movement-related signal<sup>17,18</sup>, such as corollary discharge  
68 from (pre-)motor areas, may act as a suppressive command for visual neurons to  
69 cause perceptual suppression, and maybe even in a pathway-selective manner<sup>11</sup>.

70  
71 On the other hand, perceptual saccadic suppression could alternatively, or  
72 additionally, arise as a result of the visual consequences of retinal image shifts  
73 caused by eyeball rotations<sup>2,20-31</sup>. After all, the early visual system, including the  
74 retina, is a highly sensitive light sensing device, and it therefore ought to capture  
75 visual transients associated with saccade-induced retinal image shifts. Such early

76 processing of visual transients could modulate the retinal output, jumpstarting an  
77 image processing cascade to mediate perceptual saccadic suppression.

78

79 In this study, rather than arguing either strictly for or strictly against one of the above  
80 two seemingly contrasting hypotheses, we instead asked to what extent they might  
81 interact with and support each other for the ultimate service of perception. We were  
82 specifically motivated by the fact that the very first visual processing stage in the  
83 brain, the retina, is not only sensitive to visual transients (such as saccade-induced  
84 image shifts), but it also possesses rich image processing circuitry that is capable, in  
85 principle, of regularizing the visual disruptions<sup>32–37</sup> caused by saccades. We therefore  
86 asked: how much of the characteristics of perceptual saccadic suppression can be  
87 explained by visual-only mechanisms? And, to the extent that there are visual-only  
88 mechanisms underlying perceptual saccadic suppression, would the first neural locus  
89 for such visual-only mechanisms indeed be the very first stage of visual processing in  
90 the brain, the retina?

91

92 We used a multi-disciplinary approach in which we experimentally mimicked the  
93 visual consequences of saccades and recorded neural activity from *ex vivo* retinae of  
94 different animal models. We also measured perceptual reports in humans using both  
95 real saccades as well as simulated saccade-like image displacements. We found a  
96 surprisingly far-reaching contribution of visual processing mechanisms to perceptual  
97 saccadic suppression, starting in the retina, without the need to invoke explicit motor-  
98 based suppression commands. Intriguingly, the role of motor-based commands  
99 seems to be the opposite of what has been proposed before. Rather than sending an  
100 explicit suppressive command to reduce the sensitivity of the visual system, motor-

101 based commands instead seem to minimize the duration of visually-derived saccadic  
102 suppression.

103

## 104 **Results**

### 105 *Perceptual saccadic suppression depends on image content*

106 We first asked human subjects to generate saccades across textured backgrounds,  
107 akin to how saccades may be made in real life. Subjects viewed coarse or fine  
108 textures (Fig. 1a, Methods and Supplementary Fig. 1). Starting from one of four  
109 locations on the display, subjects made 4.8 deg saccades towards display center  
110 (Fig. 1a, left). We varied saccade onset and endpoint locations, as well as texture  
111 images, across trials to avoid subjects remembering specific texture patterns  
112 (Methods). At a random time, a luminance pedestal (probe flash) was added to the  
113 texture background, for one display frame (approximately 12 ms; Methods), at one of  
114 four locations relative to the saccade endpoint (7 deg eccentricity; Fig. 1a, right). At  
115 trial end, the subjects were asked to localize the probe flash, and we analyzed how  
116 well they did so. We took care to ensure that the retinal region of flash location was  
117 stimulated with the background texture (rather than the edge of the monitor or the  
118 black surround of the dark laboratory) throughout any given trial (Methods). We also  
119 ensured that the size of the probe flash was larger than the image blobs in the coarse  
120 texture, such that average luminance variation within each flash was matched across  
121 trials and textures. Coarse and fine textures had blobs that approximated the sizes of  
122 retinal ganglion cell (RGC) or retinal bipolar cell receptive fields, respectively, at the  
123 retinal flash locations<sup>38</sup> (Methods).

124

125 For both coarse and fine textures, subjects were strongly impaired in their ability to  
126 localize flashes presented peri-saccadically, thus experiencing strong perceptual

127 saccadic suppression (Fig. 1b, c). However, there was a clear dependence of the  
128 suppression on the background visual image: saccadic suppression started  
129 significantly earlier and recovered significantly later with saccades across coarse  
130 rather than fine textures (Fig. 1d; the highlighted time intervals show significant  
131 differences between coarse and fine textures at a p-value of  $p < 0.001$ , cluster-based  
132 random permutation test<sup>39,40</sup>; Methods). Moreover, the peak amount of suppression  
133 was stronger with the coarse textures (Fig. 1d). However, for both coarse and fine  
134 textures, performance reached a floor effect in this version of the experiment,  
135 masking an even larger difference (see below and Fig. 2). This dependence of  
136 perceptual saccadic suppression on background texture was robust across individual  
137 subjects (Supplementary Fig. 2a; also see Supplementary Fig. 4 for further individual  
138 subject effects).

139

140 To rule out the possibility that the difference in perceptual saccadic suppression  
141 profiles between the coarse and fine textures was due to the flashes being simply  
142 easier to see over the fine texture, we performed a control experiment in which we  
143 collected full psychometric curves of perceptual performance during simple fixation.  
144 We found that, without any saccades, the visibility of the probe flashes was identical  
145 over coarse and fine background textures (Supplementary Fig. 3a, b). Therefore, the  
146 image dependence of the results of Fig. 1 was related to saccadic suppression itself  
147 and not to the baseline visibility of brief flashes over the different textures. Similarly,  
148 we carefully analyzed eye movement properties, and we found that the results of Fig.  
149 1 were also not due to different saccade kinematics for the different textures  
150 (Supplementary Fig. 3c, d).

151

152 To further explore the differences in suppression profiles that we observed in Fig. 1,  
153 we next employed a more sensitive procedure to evaluate perceptual thresholds.  
154 Specifically, we repeated the same experiment of Fig. 1 on five subjects (three of  
155 whom being the same as those who participated in the earlier experiment). This time,  
156 we collected full psychometric curves of perceptual performance (Methods; similar to  
157 Supplementary Fig. 3a, b). Because collecting full psychometric curves for each  
158 texture and each time point relative to saccade onset would be a very data-intensive  
159 endeavor, we reduced the number of time points relative to saccade onset at which  
160 we probed perception. We also expedited the data collection by implementing a real-  
161 time saccade detection algorithm, described by Chen and Hafed<sup>41</sup>, and we presented  
162 the probe flash at four distinct times after online saccade detection. The four flash  
163 times were strategically chosen to evaluate peak suppression (shortly after saccade  
164 onset) as well as the time course of recovery after a saccade. We used an adaptive  
165 QUEST<sup>42</sup> procedure to estimate the perceptual threshold per condition and flash time  
166 (Methods), with the perceptual threshold (for the purposes of QUEST) being defined  
167 as the flash contrast value resulting in 62.5% correct performance. Besides the  
168 QUEST procedure, we also collected more trials showing different flash contrast  
169 levels relative to estimated perceptual threshold, in order to obtain full psychometric  
170 curves. The results are shown in Fig. 2, and they match those of Fig. 1: relative to the  
171 baseline psychometric curves of flash visibility long after saccades (dashed curves),  
172 peri-saccadic psychometric curves were clearly shifted towards higher contrast  
173 thresholds (Fig. 2a-d), consistent with Fig. 1. More importantly, with the more  
174 sensitive approach of full psychometric curves, we could clearly see that perceptual  
175 saccadic suppression was much stronger for coarse than fine textures at peak  
176 suppression; that is, perceptual thresholds (defined as luminance increments  
177 required for a specific correct performance level; Methods) near peak suppression

178 were higher for coarse than fine textures (Fig. 2e). Supplementary Fig. 4 shows the  
179 corresponding individual subject psychometric curves and perceptual thresholds.

180

181 In summary, we found that perceptual saccadic suppression was associated with a  
182 visual component directly influencing its strength and time course: saccades across  
183 coarse textures were associated with both stronger and longer-lasting perceptual  
184 suppression than saccades across fine textures, even when the kinematics of the  
185 eye movements (and thus the underlying motor commands) did not differ across the  
186 two conditions.

187

### 188 *Perceptual saccadic suppression originates in the retina*

189 To test if this visual component of perceptual saccadic suppression originates in the  
190 retina, we isolated mouse and pig retinæ and performed multi-electrode array  
191 recordings (Methods). We continuously exposed each retina to coarse and fine  
192 textures, matched to ganglion and bipolar cell receptive field sizes in the recorded  
193 species (Methods, Supplementary Fig. 1). We rapidly translated the textures globally  
194 to simulate saccade-like image displacements (Fig. 3a, Methods). Such  
195 displacements can robustly activate RGCs, as is evident from the example mouse  
196 RGC shown in Fig. 3b. In fact, most recorded RGCs (mouse: 83% of 1,423 cells, pig:  
197 73% of 394 cells) responded robustly to texture displacements, indicating that  
198 saccade-induced visual transients during active gaze behavior can constitute strong  
199 signals to the retina. Next, at different times relative to texture displacements, we  
200 introduced a luminance pedestal (probe flash) to the entire texture for 16 or 33 ms,  
201 similar in principle to the perceptual experiments of Figs. 1, 2. Such flashes, when  
202 presented in isolation (that is, temporally removed from the texture displacement),  
203 elicited responses in a sizable fraction of RGCs (baseline response; mouse: 688 of

204 1,423 RGCs; pig: 228 of 394 RGCs). This allowed us to evaluate the consequences  
205 of texture displacements on flash responses in these cells, in a way that is  
206 conceptually similar to the experiments in Figs. 1, 2, in which we evaluated the  
207 consequences of saccades on flash perception. For example, the same RGC of Fig.  
208 3b showed much suppressed neural responses to the flash when it was presented  
209 immediately after texture displacements compared to the baseline condition (Fig. 3c,  
210 d). This suppression of flash-induced responses (Fig. 3d) looks remarkably similar to  
211 suppression of visual responses in, say, macaque superior colliculus for stimuli  
212 presented after real saccades<sup>7,14,43</sup>. Thus, neuronally, there does exist “saccadic  
213 suppression” of visual sensitivity at the very first stage of visual processing in the  
214 brain, the retina, and it looks qualitatively indistinguishable from saccadic  
215 suppression at downstream neural sites<sup>7,14,43</sup> and, indeed, perception (Figs. 1, 2).  
216  
217 Importantly, retinal “saccadic suppression” strongly depended on background texture  
218 (Fig. 3e), exactly like in our human experiments (Figs. 1, 2). Specifically, we  
219 quantified retinal “saccadic suppression” by calculating a neuronal modulation index,  
220 defined as  $(r_d - r_b)/(r_d + r_b)$ . Here,  $r_d$  is the response strength to the probe flash  
221 presented with a delay  $d$  relative to the texture displacement onset, and  $r_b$  is the  
222 response strength in baseline (Methods). This modulation index is, by definition,  
223 negative for suppressed flash-induced responses. The great majority of RGCs were  
224 strongly suppressed during and after texture displacements, with gradual recovery  
225 afterwards (Fig. 3e; Supplementary Fig. 5 shows the underlying population data), and  
226 the suppression was more pronounced for coarse than fine textures (Fig. 3e;  
227 Supplementary Fig. 5). These results are consistent with the dependence of human  
228 perceptual saccadic suppression on background texture statistics shown above  
229 (Figs. 1, 2), suggesting that this dependence starts already in the retina.

230

231 We also found that retinal “saccadic suppression” was a robust phenomenon across  
232 many different RGCs, with diverse properties (Supplementary Fig. 6). Further, it  
233 occurred both in mouse (Fig. 3e, left) and pig (Fig. 3e, right) retinae, two mammalian  
234 species with different native oculomotor behavior, different lifestyles, and different  
235 eye sizes. Thus, our results so far suggest that perceptual saccadic suppression  
236 (Figs. 1, 2), including its dependence on background texture statistics, most likely  
237 originates in the retina (Fig. 3), being the outcome of very general retinal-circuit  
238 mechanisms that are conserved across species.

239

#### 240 *Stimulus-stimulus interactions underlie retinal suppression*

241 To understand the underlying mechanisms for retinal “saccadic suppression” in more  
242 detail, we explored its properties using different analyses and additional stimulus  
243 manipulations. First, we wondered about neural activity saturation, given that  
244 saccade-like texture displacements before flash onset could activate RGCs (e.g. Fig.  
245 3b). Specifically, if RGC activity is elevated by the texture displacement alone  
246 (because it was a visual transient), then any subsequent flash-induced response  
247 could have caused the cell to reach activity saturation. However, this was not  
248 sufficient to explain our results. For example, we observed that suppression often  
249 also occurred in RGCs that did not respond strongly to the texture displacements in  
250 the first place (Fig. 4a).

251

252 Second, we investigated whether retinal “saccadic suppression” critically depended  
253 on particular saccade-like profile speeds. In the original experiments of Fig. 3, we  
254 simulated saccade-induced image translation speeds to the best of our abilities  
255 (given the sampling rate of our display; Methods). However, if we replaced the

256 original translation over 100 ms with a sudden texture jump from the start- to end-  
257 position in one display update (an infinite-speed texture jump), then the same  
258 suppression took place, with similar dependence on texture statistics (Fig. 4b).  
259 Similarly, in yet another manipulation, when we presented first a flash and then a  
260 texture displacement, then the second response (now to the texture displacement)  
261 was suppressed (Fig. 4c). This suggests that retinal “saccadic suppression” can be  
262 explained by general stimulus-stimulus interaction effects in the retina. As a result, it  
263 is a phenomenon that is unlikely to critically depend, at least qualitatively, on the  
264 specific oculomotor repertoire of either mice, pigs, or humans.

265

266 The most compelling evidence for stimulus-stimulus interactions underlying retinal  
267 “saccadic suppression” came from experiments when we replaced the texture  
268 displacements with a structure-free luminance step (Fig. 4d). Specifically, instead of  
269 a background texture and a displacement of this texture, we exposed the retina to a  
270 uniform gray background and introduced a sudden uniform luminance increase or  
271 decrease as the visual transient. This luminance step was either of high contrast (+/-  
272 0.20 to 0.40 Michelson contrast) or low contrast (+/- 0.03 to 0.15 Michelson contrast)  
273 (Methods). The probe flash then followed the luminance step as in the original  
274 experiments. We found that responses to probe flashes were indeed suppressed  
275 after luminance steps. This suppression was stronger after high-contrast visual  
276 transients than after low-contrast visual transients. Interestingly, the suppression  
277 after high- and low-contrast luminance steps was quantitatively similar to the  
278 suppression after coarse and fine texture displacements, respectively (e.g. Fig. 3),  
279 both for the time course of suppression and its strength (Fig. 4e). Presumably,  
280 moving the larger blobs of a coarse texture across the retina would result in high-  
281 contrast changes within individual retinal receptive fields (e.g. from a bright blob in a

282 receptive field before the texture displacement to a dark blob after the displacement),  
283 while the smaller blobs in the fine texture would be spatially averaged within  
284 receptive fields, resulting in low-contrast changes.

285

286 When we next performed human psychophysical experiments mimicking the  
287 luminance step retinal experiments, we found remarkably congruent results (Fig. 5).  
288 Specifically, subjects maintained saccade-free fixation, and we simply changed the  
289 luminance of the homogenous background (Methods). At random times relative to  
290 the change in luminance, we presented brief probe flashes exactly like we did in Fig.  
291 1. In all subjects, we found clear perceptual suppression in response to the  
292 luminance steps. Importantly, we also found clear dependence of perceptual  
293 suppression on the contrast of the luminance change: when there was a small  
294 change in background luminance, suppression was minimal; when there was a large  
295 change in background luminance, suppression was strong and long-lasting (Fig. 5).  
296 As we discuss below, we observed perceptual suppression even for flashes *before*  
297 the background luminance changes; this matters for interpretations of pre-movement  
298 perceptual saccadic suppression (e.g. see Fig. 6 below).

299

300 Therefore, the most likely mechanism for our retinal “saccadic suppression” effect is  
301 that such suppression emerges as a result of retinal-circuit image processing that is  
302 initiated by visual transients; whether they be through texture displacements, infinite-  
303 speed texture jumps, or luminance steps (Fig. 4e). It is very intriguing that such  
304 stimulus-stimulus retinal effects may be inherited all the way deep into the brain’s  
305 visual processing hierarchy, including cortical (frontal eye field) and subcortical  
306 (superior colliculus) areas<sup>44</sup> that are also implicated in saccadic suppression<sup>7,43,45,46</sup>.

307

308 *Motor-related signals shorten visually-derived suppression*

309 In retina, we not only observed similarities to perceptual saccadic suppression (the  
310 presence of retinal suppression, and its dependence on texture statistics or  
311 luminance step contrast), but we additionally noticed that retinal “saccadic  
312 suppression” was particularly long lasting (e.g. Fig. 3e). To explore the potential  
313 perceptual implications of this observation, we next asked our human subjects to  
314 maintain fixation while we introduced saccade-like texture displacements in a manner  
315 similar to the retinal experiments of Fig. 3 (Fig. 6a, Methods); brief flashes occurred  
316 around the time of these “simulated saccades” exactly like in the first experiment  
317 (Fig. 1). This time, due to the absence of real saccades (trials with microsaccades  
318 were excluded; Methods), non-visual (motor-related) components could not influence  
319 flash-induced neural responses and their perception. Still, given the retinal results of  
320 Figs. 3, 4, we had three hypotheses on what to expect under these conditions, all of  
321 which we were able to validate: (1) strong perceptual suppression still occurred  
322 regardless of texture details (Fig. 6b, c); (2) suppression strength and duration  
323 depended on texture statistics (Fig. 6d); and (3) suppression outlasted the  
324 suppression with real saccades (Fig. 6e, f). This last point, in particular, suggests that  
325 motor-related signals associated with real saccades may act to shorten the  
326 perceptual interruption resulting from visually-induced saccadic suppression, while  
327 maintaining the putatively retinally-determined (Figs. 3, 4) dependence on image  
328 statistics. Note also that the first and third points above are consistent with earlier  
329 perceptual results shown by Diamond et al<sup>17</sup>.

330

331 In humans, we observed perceptual suppression also prior to saccade-like texture  
332 displacements<sup>20,27</sup> (Fig. 6). This was again consistently dependent on texture  
333 statistics (Fig. 6b-d; also see Fig. 7 below for additional evidence). Further, like the

334 suppression after saccade onset, this pre-saccadic perceptual suppression was also  
335 shorter during real saccades than during simulated saccades (due to later onset of  
336 suppression, Fig. 6e). Even in our retinal data, we found very slight “pre-saccadic”  
337 suppression. However, the effect size of retinal suppression before texture  
338 displacements was much smaller than after texture displacements: the strongest  
339 “pre-saccadic” retinal effect occurred at -67 ms with a median population modulation  
340 index of -0.024 ( $p = 6 \times 10^{-8}$ , Wilcoxon signed-rank test) compared to -0.55 ( $p = 3 \times$   
341  $10^{-82}$ ) for “post-saccadic” suppression at 150 ms delay (Fig. 3e, Supplementary Fig.  
342 5b). It is therefore likely that this particular phenomenon, perceptual pre-saccadic  
343 suppression (Fig. 6b-f), arises not in the retina, but from visual (not movement-  
344 command-related) processing further downstream, perhaps through backwards  
345 masking<sup>29,47</sup>. This also holds true for our perceptual experiments with background  
346 luminance steps (Fig. 5), and it can also explain why the time of peak suppression in  
347 our retinal experiments (Figs. 3, 4) may have been slightly different from the time of  
348 peak suppression with real saccades (Figs. 1, 2).

349  
350 Since the results of Fig. 6 did not explicitly report perceptual thresholds, we also  
351 repeated the same experiment again, but this time using the QUEST and full  
352 psychometric curve procedures described above for Fig. 2. In the current experiment,  
353 we again picked 4 specific time points relative to texture displacement onset for  
354 calculating perceptual thresholds (Methods). Like in the case of Fig. 2, we chose  
355 these 4 time points strategically to highlight perceptual threshold elevations at  
356 maximal suppression and also to highlight differences between coarse and fine  
357 textures. We also explicitly sampled a negative time point close to texture  
358 displacement onset, such that we could fill in the gap in the negative time courses  
359 shown in Fig. 6. The net conclusion (Fig. 7) was the same as that in Fig. 6. There

360 was robust elevation of perceptual thresholds before, during, and after the texture  
361 displacements. Most importantly, the elevation was much stronger and longer-lasting  
362 (both before and after texture displacements) for coarse than for fine textures. The  
363 effect was also robust across individual subjects (Supplementary Fig. 7).

364

365 Therefore, the long-lasting suppression effects that we observed in RGCs (Figs. 3, 4)  
366 were not an idiosyncrasy of the *ex vivo* electrophysiological procedures that we used,  
367 but they were reflected in the longer duration of perceptual suppression after  
368 simulated saccades. Importantly, they were indicative of a potential shortening of  
369 visually-derived suppression in association with real saccades.

370

371 *Visually-derived suppression underlies even more phenomena*

372 Our results so far suggest that visual contributions can go a very long way in  
373 explaining properties of perceptual saccadic suppression (e.g. the presence of  
374 suppression, and the dependencies on image content), without the need for invoking  
375 mechanisms related to motor commands. We therefore wondered whether such  
376 contributions can also explain classic suppression phenomena in experiments when  
377 uniform, rather than textured, backgrounds are used. One such robust phenomenon  
378 has been the selective suppression of low spatial frequencies. In a classic study by  
379 Burr et al<sup>11</sup>, subjects viewed briefly flashed Gabor gratings over a uniform  
380 background. Around the time of saccades, visibility of low-spatial frequency gratings  
381 was suppressed much more strongly than of high-frequency gratings, and this was  
382 interpreted as a motor-related influence on magnocellular pathways<sup>17,18</sup>. Still,  
383 convincing neural mechanisms for this phenomenon remain elusive<sup>7,22,30,31,48–53</sup>. Can  
384 the strong prominence of visual contributions to saccadic suppression revealed in our  
385 results so far also be extended to account for this classic phenomenon? In other

386 words, is the selective suppression of low spatial frequencies around the time of  
387 saccades<sup>11</sup> intrinsically a visual, rather than motor, phenomenon?

388

389 The answer lies in considering this phenomenon from the perspective of visual input  
390 during such experiments: saccades across a uniform background invariably involve  
391 moving the image of the video monitor (or other form of display) in visual coordinates.  
392 Therefore, the image of any edge discontinuity associated with the display monitor  
393 (or with the surrounding cardboard paper around it<sup>11</sup>) will invariably move across the  
394 retina because of the saccade. This allows us to ask if one can replicate selective  
395 suppression of low spatial frequencies<sup>11</sup> without any saccades at all, solely based on  
396 the visual flow experienced during such experiments.

397

398 We first replicated the classic phenomenon itself. Our subjects localized briefly  
399 flashed vertical Gabor gratings with different spatial frequencies (Methods); the  
400 flashes occurred peri-saccadically as in Fig. 1a. Here, however, the screen was a  
401 homogeneous gray, like in the classic experiment, with the exception of a surround  
402 region showing a stationary texture (the coarse texture used in our earlier  
403 experiments, Fig. 8a). We call the large homogeneous central region of the screen  
404 (diameter: 20 deg) the “virtual monitor”. The outcome confirmed the classic findings:  
405 Fig. 8b (left) shows localization performance for flashed gratings around saccade  
406 onset, compared to flashes without saccades (and without any other display  
407 transients; Methods), and Fig. 8b (right) plots the ratio of those percepts as a  
408 visualization aid. Perception of low spatial frequency gratings was selectively  
409 suppressed (relevant statistics are shown in Fig. 8; full time courses of these effects  
410 are shown in Supplementary Figs. 8, 9). These results are consistent with the classic  
411 phenomenon<sup>11</sup>.

412

413 The presence of the textured surround allowed us to next isolate the effects of visual  
414 flow during these experiments. In separate trials, we asked subjects to fixate, and we  
415 presented saccade-like image motion. For example, in order to simulate a real  
416 saccade from the lower right corner to display center (Fig. 8a), the virtual monitor  
417 moved together with its textured surround from the top left corner towards display  
418 center (Fig. 8c). We then briefly presented the same Gabor gratings as in Fig. 8a, b.  
419 Relative to fixation position, this experiment was comparable to the situation with real  
420 saccades: there was a uniform background against which a brief Gabor grating was  
421 flashed. And, indeed, we observed the same selective suppression of low spatial  
422 frequencies despite the absence of saccades (Fig. 8d). Moreover, again consistent  
423 with our results from Figs. 1-7, the suppression with simulated saccades lasted  
424 longer than with real saccades (robust selective suppression in Fig. 8d occurred even  
425 84 ms after simulated saccades; Supplementary Figs. 8, 9). Similar results were  
426 obtained with a uniform black surround around the virtual monitor, as might be the  
427 case in typical laboratory settings (Supplementary Fig. 10). Therefore, visual  
428 mechanisms account even for the results of Burr et al<sup>11</sup> and similar experiments<sup>7</sup>  
429 using uniform backgrounds, without the need to invoke non-visual (motor-related)  
430 mechanisms.

431

432 Motivated by the differences between coarse and fine textures in Figs. 1-7, we next  
433 replaced the coarse texture around the virtual monitor (Fig. 8c) with a fine texture,  
434 and we repeated the experiments with simulated saccades (Fig. 8f). In this case,  
435 surprisingly, we observed uniform suppression of gratings of all spatial frequencies  
436 (Fig. 8f). In other words, the specific suppression of low spatial frequencies observed  
437 earlier (Fig. 8c, with saccade-like visual flow, but without eye movements) depended

438 on the visual context containing a coarse pattern in the visual surround. This led us to  
439 make a strong prediction: if saccadic suppression properties do indeed rely on visual  
440 processing, then suppression during real saccades should depend mainly on visual  
441 context, and one should be able to easily violate the classic phenomenon (namely,  
442 the specific suppression of low spatial frequencies<sup>11</sup>). This is exactly what we found  
443 (Fig. 8e): for real saccades across the virtual monitor, and with the surrounding visual  
444 context being a fine rather than coarse texture, we observed perceptual suppression  
445 for all gratings, abolishing suppression selectivity for low spatial frequencies. In all  
446 cases, the effects were not explained by motor variability across surround texture  
447 conditions (Supplementary Fig. 3e, f).

448

449 All of these observations were further confirmed when we repeated the same  
450 experiments but now collecting full psychometric curves (Methods), similar to Figs. 2  
451 and 7 above: Fig. 9 shows results for real saccades, and Fig. 10 for simulated  
452 saccades. In both cases, when there was a coarse texture in the surround,  
453 perceptual threshold was elevated (i.e., perception was suppressed) more strongly  
454 for low-spatial frequency Gabor patches. With a fine texture surround, perceptual  
455 threshold was elevated non-specifically for all probe Gabor patches.

456

457 In summary, perceptual saccadic suppression occurred in all of our experiments,  
458 either with or without real saccades, simply as a function of visual flow (Figs. 1, 2, 6-  
459 10). Simple visual transients, without the need for saccade-like stimulus kinetics,  
460 were sufficient to elicit suppression in both retina and perception (Figs. 4, 5). Such  
461 suppression quantitatively depended on scene statistics, both for full-field textures  
462 (Figs. 1, 2, 6, 7) in a manner predicted by retinal processing (Figs. 3-5), and for

463 textures limited to the surround (Figs. 8-10). Even the suppression selectivity of low  
464 spatial frequency probes<sup>11</sup> was determined by visual context (Figs. 8-10).

465

## 466 **Discussion**

467 We found that visual image processing accounts for a large component of classic  
468 perceptual demonstrations of saccadic suppression, and that such image processing  
469 occurs as early as in the very first stage of visual processing, the retina. This early  
470 neural implementation is interesting because it suggests that the image dependence  
471 of perceptual saccadic suppression that we observed (Figs. 1, 2) is derived, at least  
472 in part, from visual image processing starting in the retina. In fact, we found  
473 remarkable congruence between the image dependence of three seemingly  
474 disparate phenomena: perceptual suppression with real saccades (Figs. 1, 2),  
475 perceptual suppression with simulated saccades (texture displacements; Figs. 6, 7),  
476 and neural suppression patterns in RGCs, which carry the retinal output (Figs. 3, 4).  
477 In all cases, modifying the background texture statistics resulted in highly predictable  
478 changes in suppression profiles. This was further corroborated when we replaced the  
479 texture displacements with simple luminance steps (instantaneous changes of  
480 background luminance) in both the retina (Fig. 4d) and perception (Fig. 5).

481

482 Key to all of our observations is the single insight that, from the perspective of visual  
483 image processing, a saccade is itself a potent stimulus to the visual system. For  
484 example, our RGCs often responded vigorously to saccade-like image displacements  
485 (Fig. 3b). Therefore, when probing perceptual sensitivity around the time of saccades  
486 using brief flashes, as in classic studies of perceptual saccadic suppression, the  
487 visual system is not only responding to the externally provided brief flashes, but it is  
488 also responding to the self-induced visual flows caused by eyeball rotations. These

489 saccade-induced rapid image shifts across the retina trigger visual mechanisms that  
490 can suppress the response to subsequent stimulation. Such suppression of neural  
491 responses is not exclusive to saccades. It instead occurs for any scenario that  
492 involves sequential visual stimulation, including visual masking paradigms<sup>2,28,29,47</sup> and  
493 double-flash paradigms<sup>44</sup>. It is therefore not surprising that the outcome is also  
494 comparable: the response to a second stimulus is suppressed by the presence of a  
495 first stimulus, be it a mask, a flash, or transients caused by saccade-induced image  
496 shifts across the retina. Indeed, our own results demonstrate that sequential visual  
497 stimulation (luminance step plus probe flash) shows qualitatively similar perceptual  
498 (Fig. 5) and retinal (Fig. 4d) suppression profiles to those seen with simulated  
499 saccades. Therefore, classic saccadic suppression paradigms, employing brief visual  
500 probes in the temporal vicinity of saccades, are essentially stimulus-stimulus  
501 paradigms from the perspective of visual flow on the retina.

502

503 Additional support for the above sentiment emerges from the time courses of  
504 stimulus-stimulus neural adaptation effects in areas like the frontal eye field and  
505 superior colliculus<sup>44</sup>. These time courses are particularly intriguing to us, primarily  
506 because they agree with our observations that retinal (Figs. 3, 4) and perceptual  
507 (Figs. 6, 7) suppression with simulated saccades had longer suppression time  
508 courses than observed with real saccades (Figs. 1, 2). Indeed, the time courses of  
509 the neural adaptation effects in the frontal eye field and superior colliculus<sup>44</sup>, and  
510 related brain areas, are similar to our observed perceptual time courses in the  
511 absence of real saccades. Given that both the frontal eye field and superior colliculus  
512 have previously been implicated in suppression with real saccades<sup>7,43,45,46</sup>, it is thus  
513 conceivable that saccadic suppression in these areas is inherited, at least partially,  
514 from the retina.

515

516 Looking forward, we believe that it is imperative to also investigate the neural  
517 mechanisms behind visual masking in much more detail. In our perceptual  
518 experiments with simulated saccades (Figs. 6, 7), we saw clear suppression of  
519 perceptual performance even when the probe flashes appeared before texture  
520 displacement. That is, perceptual localization of the probes was masked, backwards  
521 in time, by the subsequent texture displacement. In the past, pre-saccadic  
522 suppression with real saccades (e.g. Fig. 1) has sometimes been taken as evidence  
523 that perceptual saccadic suppression is fundamentally driven by motor-related  
524 signals like corollary discharge. However, our results (Fig. 6, 7) show that motor  
525 activity is not required, and a visual transient is sufficient. Even simple background  
526 luminance steps were associated with pre-step perceptual suppression (Fig. 5).  
527 These effects have been described as backwards visual masking<sup>47</sup>, but what are the  
528 underlying neural mechanisms? Such backwards masking was not present in our  
529 retinal results, certainly not as clearly as in perception, so it must emerge through  
530 visual mechanisms in other brain structures.

531

532 One possibility could be related to the fact that perception necessarily involves an  
533 interpretation of sensory evidence that is strongly dependent on priors. In the case of  
534 global retinal image motion, which is caused by eye movements in most real-world  
535 scenarios, priors could influence the percept of a flash occurring before a saccade or  
536 texture displacement. Specifically, such priors may cause perception to “omit” the  
537 pre-saccadic flash even though it evokes a strong retinal transient. This would  
538 happen exactly because of the pairing of the flash with a very likely occurrence of a  
539 saccade, interpreted as such due to the global image motion, even if its neural  
540 transient in the retina is weakened by the prior flash. This would result in a kind of

541 credit assignment problem due to a strong prior association of global image motion  
542 with saccades.

543

544 More generally, our results suggest that visual flow matters a great deal in perceptual  
545 saccadic suppression, even in paradigms that have often been taken as indication for  
546 motor-related top-down suppression (Figs. 8-10). It would be interesting in the future  
547 to further test the generalizability of this notion. We were indeed greatly surprised  
548 when we performed the experiments of Figs. 8-10, and found that the classic  
549 selective suppression of low spatial frequencies in perception around the time of  
550 saccades<sup>11</sup> can be violated in two important ways. First, the selectivity of suppression  
551 can be abolished with a simple change of visual context. Second, the same selective  
552 suppression of low spatial frequencies can be obtained without saccades at all. Thus,  
553 with or without saccades, either selective or nonselective suppression could occur as  
554 a function of visual flow. In hindsight, this might shed light on a somewhat surprising  
555 recent finding in superior colliculus neurons<sup>7</sup>. There, using essentially the same  
556 paradigms, it was found that only one type of superior colliculus visually-responsive  
557 neurons (so-called visual-motor neurons) exhibited selective suppression of low  
558 spatial frequency sensitivity as in the classic perceptual phenomenon<sup>7</sup>. The other  
559 type of visually-responsive superior colliculus neurons (visual-only neurons) showed  
560 mild suppression but, critically, no selectivity for spatial frequency<sup>7</sup>. These two types  
561 of neurons occupy different laminae of the superior colliculus and have different  
562 patterns of lateral interactions from across the visual field representation of this  
563 structure<sup>54</sup>. It is now very conceivable, in light of our current results (Figs. 8-10), that  
564 both patterns of suppression (selective or not) may be embedded simultaneously in  
565 these different neuronal populations with specific circuitry and tuning for visual  
566 peripheral contexts.

567

568 Finally, it should be emphasized that motor-related mechanisms still likely play an  
569 important role in perceptual saccadic suppression. In fact, such mechanisms seem to  
570 be equally important as the visual mechanisms, since motor-related mechanisms  
571 appear to shorten pre- and post-saccadic suppression originating from visual  
572 processing (Fig. 6), and might therefore minimize the duration of saccade-induced  
573 disruptions. Indeed, there is evidence for post-saccadic enhancement of excitability  
574 in a variety of cortical areas<sup>55-57</sup>. It would be interesting to further investigate how  
575 such neural enhancement may contribute to the shortened time courses of  
576 perceptual saccadic suppression that we observed (e.g. Fig. 6e, f). Furthermore,  
577 besides just suppression, saccades are also associated with “omission”, the lack of  
578 awareness of intra-saccadic background image motion<sup>23,58</sup>. It would, therefore, also  
579 be interesting to study the neural mechanisms through which strong neural transients  
580 in the retina in association with saccades (Fig. 3b) are perceptually “omitted” to give  
581 the illusion of continuous perception across saccades. More intriguingly, saccades  
582 also cause spatial updating of visual reference frames (due to the image shifts that  
583 they cause). Information contained in the motor command itself is likely critical for  
584 adjustments of spatial receptive fields across saccades, which have been observed  
585 in parietal and frontal cortices<sup>59,60</sup>. Our findings leave open the possibility, however,  
586 that trans-saccadic image flow might play a role in this phenomenon as well.

587

588 **Methods**

589 *Ethics approvals*

590 We performed electrophysiological experiments on *ex vivo* mouse and pig retinae as  
591 well as non-invasive perceptual experiments on human subjects.

592

593 Animal use was in accordance with German and European regulations, and animal  
594 experiments were approved by the Regierungspräsidium Tübingen.

595

596 Human subjects provided written, informed consent, and they were paid 8-15 Euros  
597 per session of 45-90 minutes each. Depending on the experiment, each subject was  
598 measured for 2-10 sessions (detailed trial and session numbers are provided below).

599 Human experiments were approved by ethics committees at the Medical Faculty of  
600 Tübingen University, and they were in accordance with the Declaration of Helsinki.

601

602 *Retina electrophysiology laboratory setup*

603 We used retinae extracted from *PV-Cre x Thy-S-Y* mice (*B6;129P2-Pvalb<sup>tm1(cre)Arbr/J</sup>*  
604 *x C57BL/6-tg (ThystopYFPJS)*), which are functionally wild type<sup>61–63</sup>. 23 retinae from  
605 7 male and 15 female mice (3-12 months old) were used. We also replicated  
606 experiments on pig retinae obtained from domestic pigs after they had been  
607 sacrificed during independent studies at the Department of Experimental Surgery in  
608 our Medical Faculty. We used 9 pig retinae.

609

610 We housed mice on a 12/12 h light/dark cycle, and we dark adapted them for 4-16 h  
611 before experiments. We then sacrificed them under dim red light, removed the eyes,  
612 and placed eyecups in Ringer solution (in mM: 110 NaCl, 2.5 KCl, 1 CaCl<sub>2</sub>, 1.6

613 MgCl<sub>2</sub>, 10 D-glucose, and 22 NaHCO<sub>3</sub>) bubbled with 5% CO<sub>2</sub> and 95% O<sub>2</sub>. We  
614 removed the retina from the pigment epithelium and sclera while in Ringer solution.

615

616 Pigs were anesthetized using atropine, azaperone, benzodiazepine (midazolam), and  
617 ketamine, and then sacrificed with embutramide (T61). Before embutramide  
618 administration, heparin was injected. The pigs were dark-adapted for 15-20 min  
619 before sacrifice. Immediately after sacrifice, the eyes were enucleated under dim red  
620 light, and the cornea, lens, and vitreous were removed. Eyecups were kept in CO<sub>2</sub>-  
621 independent culture medium (Gibco) and protected from light. We transported  
622 eyecups to our laboratory and cut pieces from mid-peripheral or peripheral retinae.

623

624 We recorded retinal ganglion cell (RGC) activity using either low or high-density  
625 multi-electrode arrays (MEAs). The low-density setup consisted of a perforated 60-  
626 electrode MEA (60pMEA200/30ir-Ti-gt, Multichannel Systems, Reutlingen, Germany)  
627 having a square grid arrangement and 200 μm inter-electrode distance. We mounted  
628 an isolated retina on a nitrocellulose filter (Millipore) with a central 2 x 2 mm hole.  
629 The mounted retina was placed with the RGC side down into the recording chamber,  
630 and good electrode contact was achieved by negative pressure through the MEA  
631 perforation. We superfused the tissue with Ringer solution at 30-34 °C during  
632 recordings, and we recorded extracellular activity at 25 kHz using a USB-MEA-  
633 system (USB-MEA 1060, Multichannel Systems) or a memory-card based system  
634 (MEA1060, Multichannel Systems). More details are provided in Reinhard et al<sup>64</sup>.

635

636 The high-density MEA setup consisted of either a HiDens CMOS MEA<sup>65</sup> (developed  
637 by the lab of Andreas Hierlemann, Basel, Switzerland) or a MaxOne system<sup>66</sup>  
638 (Maxwell Biosystems, Basel, Switzerland). The HiDens CMOS MEA featured 11,011

639 metal electrodes with inter-electrode (center-to-center) spacing of 18  $\mu\text{m}$  placed in a  
640 honeycomb pattern over an area of 2 x 1.75 mm. Any combination of 126 electrodes  
641 could be selected for simultaneous recording. The MaxOne MEA featured 26,400  
642 metal electrodes with center-to-center spacing of 17.5  $\mu\text{m}$  over an area of 3.85 x 2.1  
643 mm. In this system, up to 1,024 electrodes could be selected for simultaneous  
644 recordings. For each experiment, a piece of isolated retina covering almost the entire  
645 electrode array was cut and placed RGC-side down in the recording chamber. We  
646 achieved good electrode contact by applying pressure on the photoreceptor side of  
647 the retina by carefully lowering a transparent permeable membrane (Corning  
648 Transwell polyester membrane, 10  $\mu\text{m}$  thick, 0.4  $\mu\text{m}$  pore diameter) with the aid of a  
649 micromanipulator. The membrane was drilled with 200  $\mu\text{m}$  holes, with center-center  
650 distance of 400  $\mu\text{m}$ , to improve access of the Ringer solution to the retina. We  
651 recorded extracellular activity at 20 kHz using FPGA signal processing hardware and  
652 custom data acquisition software.

653

654 In total, we performed 36 recordings, 24 from mouse and 12 from pig retina. 15 of the  
655 36 recordings were done using low-density MEAs. Once a basic experimental  
656 protocol was established, we shifted to HiDens CMOS MEA providing much higher  
657 throughput. 12 experiments were done using this setup. We upgraded to the MaxOne  
658 MEA for even higher throughput and did our final 9 recordings using this setup.

659

660 We presented light stimuli to the retinal piece that was placed on the MEA using a  
661 DLP projector running at 60 Hz (Acer K11 for low-density MEA experiments and  
662 Lightcrafter 4500 for high-density MEA experiments). 60 Hz is above the flicker  
663 fusion frequency of both mouse and pig retinae; therefore, the framerate of these

664 projectors was adequate for our purposes. The Acer K11 projector had a resolution  
665 of 800 x 600 pixels covering 3 x 2.25 mm on the retinal surface. Lightcrafter 4500  
666 had a resolution of 1280 x 800 pixels, extending 3.072 x 1.92 mm on the retinal  
667 surface. We focused images onto the photoreceptors using a condenser (low-density  
668 MEA recordings, illumination from below) or a 5x objective (high-density MEAs,  
669 illumination from above). In each case, the light path contained a shutter and two  
670 motorized filter wheels with a set of neutral density (ND) filters (Thorlabs NE10B-A to  
671 NE50B-A), having optical densities from 1 (ND1) to 5 (ND5). Light intensity was  
672 adjusted to be in the mesopic range.

673

674 We measured the spectral intensity profile (in  $\mu\text{W cm}^{-2} \text{nm}^{-1}$ ) of our light stimuli with a  
675 calibrated USB2000+ spectrophotometer (Ocean Optics) and converted the physical  
676 intensity into a biological equivalent of photoisomerizations per rod photoreceptor per  
677 second ( $\text{R} \cdot \text{rod}^{-1} \text{s}^{-1}$ ), as described before<sup>63</sup>. Light intensities of the projector output  
678 covered a range of 3 log units (i.e. 1,000-fold difference between black and white  
679 pixels, over an 8-bit range). We linearized the projector output, and we used only  
680 grayscale images of limited contrast, spanning at most the range from 0 to 120 in the  
681 8-bit range of the projector (see stimulus description below for details). Absolute light  
682 intensities were set to the mesopic level, where a stimulus intensity of '30' in our 8-bit  
683 DLP projector scale (0-255) corresponded to 225 to 425  $\text{R} \cdot \text{rod}^{-1} \text{s}^{-1}$ , depending on the  
684 experimental rig used for the experiment (i.e. different DLP projectors and MEAs).  
685 We pooled all data from the different rigs because separate individual analyses from  
686 the individual setups revealed no effects of recording conditions in the different  
687 setups.

688

689 *Human psychophysics laboratory setup*

690 We used a similar laboratory setup to our recent experiments<sup>40,67,68</sup>. Briefly, subjects  
691 sat in a dark room 57 cm in front of a CRT monitor (85 Hz refresh rate; 41 pixels per  
692 deg resolution) spanning 34.1 x 25.6 deg (horizontal x vertical). Head fixation was  
693 achieved with a custom head, forehead, and chin rest<sup>67</sup>, and we tracked eye  
694 movements (of the left eye) at 1 kHz using a video-based eye tracker (EyeLink 1000,  
695 SR Research Ltd, Canada). Gray and texture backgrounds (e.g. Figs. 1, 6, 8-10)  
696 were always presented at an average luminance of 22.15 cd m<sup>-2</sup>, and the monitor  
697 was linearized (8-bit resolution) such that equal luminance increments and  
698 decrements were possible around this average for textures and gratings. For the  
699 experiments in which we used luminance steps of the background as the visual  
700 transients replacing saccade-induced transients (Fig. 5), details of the luminances  
701 used are presented below with the experimental procedures.

702

703 Human Experiment 1 (Fig. 1) was performed by eight subjects (two female) who  
704 were 21-25 years old. All subjects were naïve to the purposes of the experiment,  
705 except for subject MB (an author). For Human Experiment 2, the “simulated saccade”  
706 version of Human Experiment 1 (Fig. 6), six of the same subjects participated. A  
707 control experiment for testing visibility of flashes without saccades and without  
708 saccade-like texture displacements (Supplementary Fig. 3a, b) was performed by six  
709 of the same subjects plus one non-naïve subject, ZH (another author).

710

711 In the variants of Human Experiments 1 and 2 in which we collected full psychometric  
712 curves and perceptual thresholds (e.g. Figs. 2, 7 and Supplementary Figs. 4, 7), five  
713 subjects (24-29 years old; one female) participated. Three of these subjects were the  
714 same as those who performed Human Experiments 1 and 2 above, confirming that

715 both variants of the experiments (either with a fixed flash contrast or with full  
716 threshold calculations) allowed similar conclusions.

717

718 In the control experiment (Fig. 5) mimicking the retinal results of Fig. 4d, we collected  
719 data from 5 subjects (25-29 years old; 2 female). 2 of these subjects were the same  
720 as those who performed all experiments.

721

722 Human Experiment 3 tested suppression selectivity for low spatial frequencies (Fig.  
723 8). Six subjects (three females, 23-25 years old) participated, and only subject MB  
724 was non-naïve. Three subjects had also participated in Human Experiments 1 and 2  
725 and most of their control versions above. A control version of Human Experiment 3  
726 was also performed with black surrounds (Supplementary Fig. 10). This control  
727 experiment was performed by the same subjects that participated in Human  
728 Experiment 3.

729

730 We also ran a variant of Human Experiment 3 describing full psychometric curves of  
731 perceptual detectability (Figs. 9, 10). For each of the real (Fig. 9) or simulated (Fig.  
732 10) variants, we ran 4 subjects (24-29 years old; 1 female; 3 being the same as those  
733 who performed the experiments of Figs. 8).

734

735 Across all experiments, we ensured that the same subjects performed real and  
736 “simulated” saccade versions of a given paradigm so that we could make meaningful  
737 comparisons between these two eye movement conditions.

738

739 *Coarse and fine textures*

740 We created coarse and fine textures (Supplementary Fig. 1a) by convolving a  
741 random binary (i.e. white or black) pixel image with a two-dimensional Gaussian  
742 blurring filter<sup>69</sup> with the kernel

$$743 \quad G(x, y) = e^{-\frac{(x^2+y^2)}{2\sigma^2}}$$

744 The parameter  $\sigma$  of the kernel influenced the amount of blurring. This resulted in  
745 textures having effectively low-pass spectral content (Supplementary Fig. 1b) with a  
746 cutoff frequency ( $f_c$ ) depending on  $\sigma$ . As we describe below, we picked cutoff  
747 frequencies for coarse and fine textures that resulted in dark and bright image blobs  
748 approximating the receptive field sizes of RGCs (for coarse textures) and retinal  
749 bipolar cells (for fine textures). In other words, for a given species, coarse textures  
750 matched the resolution of RGCs, and fine textures matched the resolution of one  
751 processing stage earlier, the retinal bipolar cells.

752  
753 For the *ex vivo* experiments with mouse and pig retinae, we assumed receptive field  
754 diameters for RGCs of at least 150  $\mu\text{m}$  (Supplementary Fig. 1c; the parameter  $\sigma$  of  
755 the Gaussian blurring filter would be half that value), and diameters for bipolar cells  
756 of 25  $\mu\text{m}$  (see Zhang et al<sup>70</sup>). For human psychophysics experiments, we estimated,  
757 from the literature<sup>38</sup>, the sizes of human parasol RGC receptive fields at eccentricities  
758 >6 deg from the fovea (our flash eccentricities were 7 deg) to be around 200  $\mu\text{m}$ .  
759 This translated into a cutoff frequency of  $\sim 0.68$  cycles per deg (cpd) (Supplementary  
760 Fig. 1b). Bipolar cell receptive field sizes at this eccentricity were estimated to be 10  
761  $\mu\text{m}$  (corresponding to a cutoff frequency of  $\sim 13.7$  cpd), based on sizes of human  
762 midget RGC receptive fields in the fovea<sup>38</sup>. When calculating the textures, the actual  
763 value of the parameter  $\sigma$  (in pixel-dimensions) always incorporated the specific  
764 experimental magnification factor between the stimulation screen and the retinal

765 projection of the image. Calculating power spectra for coarse and fine textures  
766 confirmed that cutoff frequencies for a given species were consistent with our aimed  
767 designs described above (Supplementary Fig. 1b).

768

769 For both retinal and perceptual experiments, we normalized pixel intensities in the  
770 textures to have uniform variations in luminance around a given mean. In the retinal  
771 experiments, we used pixel intensities (from our 8-bit resolution scale) ranging from 0  
772 to 60 around a mean of 30, or ranging from 30 to 90 around a mean of 60 (see  
773 *Retina electrophysiology experimental procedures* below for when each paradigm  
774 was used). For the human experiments, textures had a mean luminance of 22.15 cd  
775 m<sup>-2</sup> with undulations in luminance in the texture within the range of 7.5-35.5 cd m<sup>-2</sup>.

776

777 Because each texture, particularly when coarse, could have patterns of dark and  
778 bright blobs that human subjects can remember or interpret as potential  
779 shapes/objects/figures, we varied the displayed texture images from trial to trial. This  
780 was also necessary to avoid afterimages. We generated sets of 20 coarse and 20  
781 fine textures, which we randomly interleaved across trials. Moreover, the textures  
782 themselves were designed to be larger than the viewable display area, allowing us to  
783 jitter the displayed sub-rectangle of each texture (within the viewable area of the  
784 display) from trial to trial (we jittered the displayed sub-rectangle within a range of 0.6  
785 x 0.6 deg in steps of 0.024 deg). This way, even fine patterns at foveal fixation  
786 locations could not be memorized by the subjects across trials.

787

788 *Retina electrophysiology experimental procedures*

789 To simulate saccades in our *ex vivo* retina electrophysiology experiments, we  
790 displaced the texture across the retina in 6 display frames (100 ms at 60 Hz refresh

791 rate). For easier readability, we sometimes refer to these saccade-like texture  
792 displacements as “saccades”. The textures were displaced in each frame by a  
793 constant distance along a linear trajectory. While each “saccade” lasted 100 ms,  
794 displacement direction was varied randomly for each “saccade” (uniformly distributed  
795 across all possible directions), and “saccade” amplitude could range from 310  $\mu\text{m}$  to  
796 930  $\mu\text{m}$  (corresponding to a velocity range of 3,100-9,300  $\mu\text{m s}^{-1}$  on the retinal  
797 surface). In visual degrees, this corresponds to a velocity range of 100-300  $\text{deg s}^{-1}$   
798 and displacement range of 10-30 deg in mice, well in the range of observed mouse  
799 saccade amplitudes<sup>71</sup>. In fact, similar to primates, mice also have oculomotor  
800 behavior, even under cortical control<sup>72</sup>. For example, they make, on average, 7.5  
801 saccade-like rapid eye movements per minute when their head is fixed<sup>71</sup> (humans  
802 make several saccades per second). We used the same retinal displacement range  
803 of 310  $\mu\text{m}$  to 930  $\mu\text{m}$  for pig retinae. To the best of our knowledge, pig oculomotor  
804 behavior has not been documented in the literature. However, with their larger  
805 eyeball sizes, our translations of the retinal image would correspond to slower  
806 saccades (e.g. small saccades in humans and monkeys), which are also associated  
807 with saccadic suppression. Moreover, we showed (Fig. 4) that retinal “saccadic  
808 suppression” is not critically dependent on the details of movement kinematics.  
809  
810 Each “trial” consisted of 39 successive sequences that each combined a “saccade”  
811 with a probe flash, as follows: there was first a “pre-saccade” fixation of 2 seconds,  
812 then a 100 ms “saccade”, followed by “post-saccade” fixation. The background  
813 texture was switched on at the beginning of each trial and was translated across the  
814 retina during each “saccade”. At a certain time from “saccade” onset (delay  $d$ , range:  
815 -177 ms to 2,100 ms), we presented a probe flash. In most cases, the probe flash

816 had a duration of 1 frame (~16 ms). We used 2 frames (~33 ms) in a subset of  
817 experiments (mouse: 161 of 688 cells analyzed for “saccadic suppression”; pig: 112  
818 of 228 cells). Results were pooled across these paradigms as they were  
819 indistinguishable. For sequences containing no probe flash, the next “saccade”  
820 happened 4 seconds after the previous one. The probe flash was a full-screen  
821 positive (“bright”) or negative (“dark”) stimulus transient. In different experiments, only  
822 a subset of possible delays was used within a given set of trials, depending on total  
823 recording time for a given retina (see below).

824

825 Bright or dark probe flashes could happen in two different ways across our  
826 experiments. The results were indistinguishable between the two ways, so we pooled  
827 results across them. Briefly, in one manipulation, the probe flash was a  
828 homogeneous bright (pixel intensity of 60 in our 8-bit projectors) or dark (pixel  
829 intensity of 0) full-screen rectangle replacing the background texture (in these  
830 experiments, the textures themselves had intensities ranging from 0 to 60 pixel  
831 intensity; see *Coarse and fine textures* above). This way, the flash contrast from the  
832 underlying background luminance was variable (e.g. a bright flash on a bright portion  
833 of a texture had lower contrast from the underlying texture than the same flash over a  
834 dark portion of the texture). In the second manipulation, the bright and dark flashes  
835 were simply luminance increments or decrements (by pixel values of 30 on our 8-bit  
836 projectors) over the existing textures (like in our human perceptual experiments).  
837 This way, local contrast relationships in the background textures were maintained. In  
838 these experiments, the textures themselves had a range of 30-90 pixel intensities  
839 and a mean pixel value of 60 (on our 8-bit projectors). 332 of 688 cells that we  
840 analyzed for “saccadic suppression” experienced such probe flashes, whereas the  
841 rest (356 cells) experienced the homogenous probe flash. For pig retina recordings,

842 we always used the homogenous framework. However, in the subset of pig  
843 experiments where the 2-frame probe flash was employed (112 of 228 RGCs), we  
844 used a high-contrast probe flash such that a bright flash would be achieved by first  
845 going completely dark in the first frame followed by the bright flash in the next frame  
846 and vice versa for a dark flash. Again, all data were pooled across these different  
847 paradigms because their outcomes were indistinguishable.

848

849 The number of trials required during a physiology experiment depended on the  
850 number of conditions that we ran on a specific day. For example, testing 7 different  
851 flash delays required 15 trials (7 with bright probe flashes, 7 with dark probe flashes,  
852 and 1 without probes). In a given experiment, we always interleaved all conditions;  
853 that is, in any one of the 15 necessary trials, each of the 39 “saccades” could be  
854 followed by a bright or a dark probe at any of the 7 delays, or no probe at all.  
855 Moreover, we repeated the total number of conditions (e.g. the interleaved 15 trials) 4  
856 times per session, and we averaged responses across repetitions. Since one trial  
857 typically lasted for 2 minutes, the example of 15 trials repeated 4 times lasted for  
858 approximately 2 hours. This was usually combined with additional conditions (e.g.  
859 other background textures), such that typical recordings lasted 10-12 hours. If the  
860 combination of conditions would have required even longer recordings in a given  
861 session, we typically reduced the number of conditions (e.g. we presented flashes at  
862 fewer delays).

863

864 We sometimes replaced the 100 ms “saccade” with an instantaneous texture jump, to  
865 test the sensitivity of retinal “saccadic suppression” (Fig. 3) to the kinematic  
866 properties of saccade-like texture displacements (Fig. 4b). Here, the texture simply  
867 jumped, in one display frame, from the pre- to the post-displacement position. All

868 other procedures were like described above. 31 RGCs were recorded with this  
869 paradigm.

870

871 In the control experiments of Fig. 4d, we used no textures at all. The screen was  
872 always a homogenous gray field, and the visual event of a "saccade" was replaced  
873 by an instantaneous step to a different gray value. The gray backgrounds had  
874 intensities between 30 and 90 (on our 8-bit projector). This instantaneous change in  
875 intensity caused either a positive contrast step (+0.03 to +0.50 Michelson contrast) or  
876 a negative contrast step (-0.03 to -0.50 Michelson contrast). A "trial" consisted of  
877 either 57 or 157 successive sequences that each combined a contrast step with a  
878 probe flash, as follows: there was first a "pre-step" fixation of 2 seconds (analogous  
879 to "pre-saccade" fixation in texture displacements), then an instantaneous switch to  
880 "post-step" fixation. At a certain time from the contrast step (delay: 17, 33, 50, 100,  
881 250, 500, 1000 or 2,000 ms), we presented a 2-frame (~33 ms) probe flash. For  
882 sequences containing no probe flash, the next contrast step happened 4 seconds  
883 after the previous one. The probe flash was either a uniform negative step of -0.33  
884 Michelson contrast ("dark") or a uniform positive step of +0.33 Michelson contrast  
885 ("bright").

886

887 Finally, we used other stimuli unrelated to the main experiments to help us  
888 characterize RGC types and other receptive field properties (e.g. response polarity,  
889 latency, transiency, and spatial receptive fields). These stimuli had the same mean  
890 intensities and intensity ranges as the textures used in each experiment. Below, we  
891 describe these stimuli for the condition in which the texture intensities ranged from 0  
892 to 60 pixel intensity (represented as grayscale RGB values in the units of our 8-bit  
893 projects). In experiments in which the textures ranged in intensity from 30 to 90, all

894 intensities reported below were shifted upward by 30. (1) Full-field contrast steps.  
895 ON steps: stepping from 0 to 30 (+1 Michelson contrast) and from 30 to 60 (+0.33)  
896 for 2 s. OFF steps: stepping from 60 to 30 (-0.33) and from 30 to 0 (-1) for 2 s. (2)  
897 Full-field Gaussian flicker, 1 minute. Screen brightness was updated every frame and  
898 was drawn from a Gaussian distribution with mean 30 and standard deviation 9. This  
899 stimulus was used to calculate the linear receptive field filters of ganglion cells  
900 through reverse correlation (spike-triggered averaging of the stimulus history). (3)  
901 Binary checkerboard flicker, 10-15 minutes. The screen was divided into a  
902 checkerboard pattern; each checker either covered an area of 55 x 55  $\mu\text{m}$ , 60 x 60  
903  $\mu\text{m}$ , or 65 x 65  $\mu\text{m}$  depending on the recording rig. The intensity of each checker was  
904 updated independently from the other checkers and randomly switched between 10  
905 and 50 or 0 and 120. This stimulus also allowed us to calculate the linear filters of  
906 cells' receptive fields.

907

### 908 *Human psychophysics experimental procedures*

909 In Human Experiment 1, we presented a coarse or fine background texture (Fig. 1)  
910 for 800-1,700 ms in every trial. Over the texture, a white fixation marker (square of  
911 7.3 x 7.3 arcmin) surrounded by a uniform gray circle of 30 min arc radius was  
912 presented at one screen location in order to guide gaze fixation onto the marker. The  
913 fixation marker was always at 4.8 deg eccentricity from display center, but its specific  
914 location was varied from trial to trial (up-right, up-left, down-right, or down-left relative  
915 to display center; 45 deg direction from horizontal). After the end of the initial interval,  
916 the fixation marker jumped to display center, instructing subjects to generate a  
917 saccade.

918

919 At a random time from the saccade instruction (47, 94, 153, 200, 247, or 507 ms), a  
920 luminance pedestal (probe flash) was applied for one display frame (~12 ms) at one  
921 of four locations relative to display center (7 deg above, below, to the right of, or to  
922 the left of center). Note that because the display was rasterized (that is, drawn by the  
923 computer graphics board from the top left corner in rows of pixels), the actual exact  
924 flash time and duration depended on the location of the flash on the display (but in a  
925 manner like other psychophysical experiments studying the same phenomenon, and  
926 also in a manner that is unlikely to affect our results). The luminance pedestal  
927 consisted of a square of 147.8 x 147.8 min arc in which we added or subtracted a  
928 value of 4.8 cd m<sup>-2</sup> to the texture pattern. Therefore, local contrast within the  
929 luminance pedestal was the same as that without the pedestal. Since all of our  
930 analyses revealed identical results whether the pedestal was a luminance increment  
931 or decrement, we combined these conditions in all analyses. At the end of the trial,  
932 subjects had to report their perceived flash location by pressing one of four buttons,  
933 corresponding to the four possible flash locations, on a hand-held response box.

934

935 Because saccadic reaction times were 156.9 +/- 3.3 ms s.e.m. across subjects, our  
936 choice of flash times above meant that we could analyze trials in which flashes  
937 appeared before or after saccade onset, allowing us to obtain full time courses (e.g.  
938 Fig. 1). Also, because of the display geometry, the retinal region that experienced a  
939 flash before, during, or after a saccade was always a region that was visually-  
940 stimulated by the texture before flash onset (rather than by the monitor edge or the  
941 black surround of the laboratory). Therefore, we maintained pre- and post-flash visual  
942 stimulation by texture background, as in the retinal experiments. We also ensured  
943 that flash locations were not coincident with saccade goal locations both  
944 retinotopically and also in display coordinates. We confirmed in separate analyses

945 that similar effects of suppression (e.g. Fig. 1) occurred for each flash location  
946 separately.

947

948 We collected 576 trials per session in this experiment. Six subjects participated in 6  
949 sessions each, and the remaining two participated in 3 or 4 sessions.

950

951 Human Experiment 2 (Fig. 6) was identical, except that the initial fixation marker was  
952 presented at display center and remained there for the entire duration of a trial.

953 Instead of instructing a saccade 800-1,700 ms after fixation marker onset, we

954 translated the entire background texture (switched on at trial onset) rapidly to

955 simulate a saccade-like image displacement. Texture displacement consisted of a 6-

956 frame translation at a speed of  $176 \text{ deg s}^{-1}$ . Note that, because of our display refresh

957 rate and geometry, this meant a slightly larger displacement (of 12.4 deg) when

958 compared to the saccade sizes in Human Experiment 1. However, we chose this

959 translation because it resulted in a sufficiently fast average speed of the

960 displacement (average speed in the real saccades of Human Experiment 1 was 160

961  $\text{deg s}^{-1}$ ). This choice is not problematic because our retinal experiments revealed that

962 visual mechanisms related to saccadic suppression were not sensitive to parameters

963 of individual motion patterns (Fig. 4b).

964

965 In this experiment, the texture displacement happened in a diagonal direction to

966 simulate the directions of saccadic displacements of Human Experiment 1 (and also

967 to dissociate the direction of motion flow from the locations of the flashes, again as in

968 Human Experiment 1). For example, the texture could move globally down-right, as

969 might be expected (in terms of image motion) if subjects made upward-leftward

970 saccades in Human Experiment 1. Also, flash times were chosen relative to the onset

971 of texture displacement from among the following values: -35, -24, 24, 47, 84, 108,  
972 141, 200, 259, 494 ms.

973

974 All subjects participated in 10 sessions each in this experiment.

975

976 We also performed a control experiment, in which there was neither a real saccade  
977 (Human Experiment 1) nor a texture displacement (Human Experiment 2), but  
978 otherwise identical to these 2 experiments. Subjects simply fixated display center,  
979 and we presented (after 1,200 to 2,400 ms from trial onset) a luminance pedestal  
980 exactly as in Human Experiments 1 and 2. To obtain full psychometric curves, we  
981 varied the luminance increment from among 6 values (Supplementary Fig. 3a, b).  
982 Subjects performed two sessions each of this experiment (600 trials per session).

983

984 To explore perceptual thresholds in a more quantitative manner for Human  
985 Experiments 1 and 2, we also performed additional real or simulated saccade  
986 experiments collecting full psychometric curves (Figs. 2, 7 and Supplementary Figs.  
987 4, 7). The logic of both additional experiments (real or simulated) was the same as  
988 that of Human Experiments 1 and 2, except that we varied the luminance of the  
989 probe flash from trial to trial (like in the above control experiment of flash visibility;  
990 Supplementary Fig. 3a, b). Because this endeavor (allowing us to measure full  
991 psychometric curves) was very data intensive, we reduced the time samples relative  
992 to saccade onset or texture displacement onset at which we probed perceptual  
993 performance. For the experiment with real saccades, we used an automatic  
994 procedure to detect saccade onset in real time based on eye velocity, as described  
995 by Chen and Hafed<sup>41</sup>. We then presented the probe flash at 42, 65, 88, or 148 ms  
996 after saccade detection. These times were chosen because they covered intervals of

997 maximum perceptual saccadic suppression as well as recovery, allowing us to get a  
998 time course of perceptual threshold elevation associated with saccadic suppression.  
999 In subsequent data analyses, we confirmed that these flash times were as planned  
1000 (within the expected variability due to the asynchronous nature of saccade times  
1001 relative to display update times; Fig. 2). For the experiment with simulated saccades,  
1002 we presented the probe flash at -24, -12, 48, or 96 ms relative to the onset time of  
1003 the texture displacement. In this case, we introduced a new negative time sample to  
1004 the set (-12 ms) because the original Human Experiment 2 did not probe this  
1005 particular time (e.g. Fig. 6). It was therefore important to clarify that the time course of  
1006 perceptual suppression for simulated saccades was continuous and well-behaved,  
1007 exactly like that for real saccades.

1008

1009 In order to also estimate perceptual thresholds online in these additional  
1010 experiments, and therefore optimize the numbers of trials needed, we applied an  
1011 adaptive QUEST procedure<sup>42</sup> on each randomly interleaved condition. Specifically,  
1012 the first 40 trials of each randomly interleaved condition (e.g. flash time -24 ms and  
1013 coarse texture, or flash -12 ms time and fine texture, and so on) were part of the  
1014 QUEST procedure. The remaining trials in the session interleaved 4 additional flash  
1015 luminances per condition, which were chosen to lie around the threshold luminance  
1016 of each condition as detected by the QUEST procedure. These additional flashes  
1017 had luminances that were +/- 1 or +/- 2 times a pre-defined luminance increment for  
1018 a given condition, depending on the detected threshold and earlier pilot data.  
1019 Specifically, if the detected threshold (according to QUEST) was very low (e.g. no  
1020 suppression effect), the pre-defined luminance increment was 1 step of luminance  
1021 (dictated by the luminance resolution of our display; Supplementary Fig. 3a). That is,  
1022 the 4 additional flashes were at +/-1 and +/-2 display-determined luminance steps

1023 from the detected threshold. If the detected threshold (according to QUEST) was  
1024 high (e.g. strong suppression), we made the pre-defined luminance increment 2 or 5  
1025 display-determined luminance steps (that is, +/- 2 and +/-4 display-determined  
1026 luminance steps or +/- 5 and +/-10 display-determined luminance steps,  
1027 respectively). This allowed fitting the psychometric curves during subsequent data  
1028 analyses, including measurements from the full dynamic range of perceptual  
1029 performance. The reasoning behind this approach is as follows: depending on the  
1030 amount of perceptual saccadic suppression to be expected per condition (e.g. peak  
1031 suppression during saccades or texture displacements, or very weak suppression  
1032 during recovery), it is expected that the psychometric curves would be shifted by  
1033 different amounts from baseline depending on the particular condition (e.g. flash time  
1034 or coarse versus fine texture). Finally, also note that we only used bright flashes in  
1035 these particular experiments instead of both bright and dark flashes. In total, we  
1036 collected 240 trials per condition per subject.

1037

1038 In yet another control experiment for Human Experiments 1 and 2, we mimicked the  
1039 retinal results of Fig. 4d. Subjects fixated a central fixation spot over a gray  
1040 background. The background had one of 8 luminances (22.4, 30.24, 38.08, 45.92,  
1041 53.76, 61.6, 69.44, 77.28  $\text{cd m}^{-2}$ ). After a random initial fixation duration (similar to  
1042 Human Experiment 2), the luminance of the background was changed suddenly (in  
1043 one display frame update) to one of the remaining 7 luminances. This meant that  
1044 across trials, we had 7 total levels of contrast change in the background as our visual  
1045 transient. At one of 5 different possible times relative to the time of background  
1046 luminance change (-24, -12, 36, 72, or 108 ms), a luminance pedestal was flashed  
1047 briefly, exactly like in Human Experiments 1 and 2. We ensured that the contrast of  
1048 the flash (relative to the currently displayed background luminance) was always the

1049 same across all trials. We also ensured that baseline visibility of the pedestal in the  
1050 absence of the contrast change was at ceiling performance (see the longest sampled  
1051 time value in Fig. 5, demonstrating near perfect detection performance for all  
1052 background luminance steps). Subjects maintained fixation throughout all trials and  
1053 simply reported the locations of the brief flashes. Subjects performed 1 session,  
1054 each, of this experiment, with 1,120 trials per session.

1055

1056 In Human Experiment 3 (Fig. 8), the flashes of Human Experiments 1 and 2 were  
1057 replaced by vertical Gabor gratings having one of five different spatial frequencies  
1058 (0.41, 0.85, 1.71, 3.42, 4.56, or 6.8 cpd). The contrast of the grating (defined as the  
1059 difference between maximum and minimum luminance in the grating divided by the  
1060 sum of the same luminances) was 14.3%. Spatial phase was randomized from trial to  
1061 trial, and the  $\sigma$  parameter of the Gaussian envelope was 0.49 deg. Also, a virtual  
1062 monitor of 20 deg diameter was present at display center at the time of Gabor grating  
1063 flashes. The virtual monitor had a uniform gray luminance equal to the average of the  
1064 textures used in Human Experiments 1 and 2. Surrounding the virtual monitor, a  
1065 coarse or fine texture could be visible.

1066

1067 In one block of trials, subjects generated saccades towards display center using the  
1068 same procedures as in Human Experiment 1. Grating flash times were similar to  
1069 Human Experiment 1, and the subjects performed 6 sessions each (576 trials per  
1070 session).

1071

1072 In another block of trials, subjects maintained fixation at display center. In one third of  
1073 the trials, the virtual monitor and surrounding texture did not move. These trials  
1074 provided us with “baseline” visual performance (i.e. without saccades or virtual

1075 monitor displacements). It was necessary to have these trials because perceptual  
1076 visibility of different spatial frequencies is not equal due to the well-known human  
1077 contrast sensitivity function<sup>73</sup>. Therefore, we needed to establish “baseline” grating  
1078 visibility first and then compare the effects of saccades or saccade-like virtual monitor  
1079 displacements on such visibility. In the remaining two thirds of the trials, the virtual  
1080 monitor and surrounding texture initially appeared displaced from display center at a  
1081 location near one corner of the display and along one of the diagonal directions. After  
1082 800-1,700 ms, the virtual monitor and surrounding texture were translated rapidly  
1083 towards display center to simulate visual flow associated with the diagonal saccades  
1084 of the real-saccade version of the paradigm (the translation parameters were similar  
1085 to Human Experiment 2). Grating flashes happened 84 ms or 108 ms after virtual  
1086 monitor and texture displacement. Note that we reduced the number of flash times  
1087 here because of the larger number of conditions (5 different spatial frequencies of the  
1088 Gabor gratings) that needed to be collected. However, our data were consistent with  
1089 all other experiments in terms of recovery time courses of suppression (e.g. Figs. 1,  
1090 6, 8; Supplementary Figs. 8-10).

1091

1092 Because the initial displaced position of the virtual monitor (and texture) provided a  
1093 cue to subjects that grating onset was expected soon, and because such a cue was  
1094 not present in the one third of trials without image motion, we equalized subject  
1095 expectations across these conditions by dimming the fixation point to black from the  
1096 time of image motion onset until 200 ms after flash onset (equal timing was ensured  
1097 in the one third of trials without image motions, such that the same expectation of  
1098 grating onset was established by fixation marker dimming). The fixation marker then  
1099 disappeared, and subjects had to report flash location.

1100

1101 Subjects performed 6 sessions each of this condition, with 576 trials per session (2  
1102 subjects performed 7 and 5 sessions each instead of 6).

1103

1104 We also repeated the same experiment but with a black surround around the virtual  
1105 monitor instead of a coarse or fine texture. Note that a black surround is theoretically  
1106 equivalent to an infinitely coarse surround. We therefore expected results  
1107 conceptually similar to those with a coarse surround. Also, in this control experiment,  
1108 we randomly interleaved all trial types together in the same session (fixation with  
1109 virtual monitor displacement, real saccade, and fixation with neither virtual monitor  
1110 displacement nor saccade). This allowed us to further confirm that our results from  
1111 Human Experiment 3 were not influenced by the separate blocking of real saccade  
1112 trials and virtual monitor displacement trials.

1113

1114 We also repeated Human Experiment 3 to collect full psychometric curves, like we  
1115 did for Human Experiments 1 and 2 above. In these additional experiments, because  
1116 of the data-intensive nature of full psychometric curves, we concentrated on the 3  
1117 lowest spatial frequencies of the Gabor gratings. This was sufficient to observe  
1118 selectivity or lack of selectivity of perceptual suppression as a function of spatial  
1119 frequency (e.g. Fig. 8). More importantly, these 3 lowest spatial frequencies were  
1120 associated with ceiling baseline visibility (Fig. 8), thus simplifying interpretations of  
1121 any suppression that we would observe. The experiments were the same as Human  
1122 Experiment 3, except that the contrast of the flashed Gabor grating was varied from  
1123 trial to trial. We used a similar adaptive procedure to that used in Figs. 2, 7 to select  
1124 contrast from trial to trial, in order to optimize finding perceptual thresholds and fitting  
1125 of psychometric curves (see procedures above). We also used the same online  
1126 saccade detection algorithm as in the experiments of Fig. 2 to decide on the time of

1127 Gabor grating flash onset (see procedures above). For both real and simulated  
1128 saccade variants of these experiments, we used two times relative to the “saccade”  
1129 event, one within a period associated with strong perceptual suppression and one at  
1130 a late time point associated with perceptual recovery (see Figs. 9, 10).

1131

### 1132 *Retina electrophysiology data analysis and statistics*

1133 Low-density MEA recordings were high-pass filtered at a 500 Hz cutoff frequency  
1134 using a tenth-order Butterworth filter. We extracted spike waveforms and times using  
1135 thresholding, and we semi-manually sorted spikes using custom software. For high-  
1136 density MEA recordings, we performed spike sorting by an offline automatic  
1137 algorithm<sup>74</sup> and assessed the sorted units using UnitBrowser<sup>75</sup>. We judged the quality  
1138 of all units using inter-spike intervals and spike shape variation. Low quality units,  
1139 such as ones with high inter-spike intervals, missing spikes, or contamination, were  
1140 discarded. All firing rate analyses were based on spike times of individual units.

1141

1142 We first characterized the properties of RGCs. We calculated linear filters in  
1143 response to full-field Gaussian flicker and binary checkerboard flicker by summing  
1144 the 500-ms stimulus history before each spike. The linear filters allowed determining  
1145 cell polarity. Specifically, the amplitude of the first peak of the filter was determined. If  
1146 the peak was positively deflected, the cell was categorized as an ON cell; if  
1147 negatively deflected, the cell was an OFF cell. ON cells were later always analyzed  
1148 with respect to their responses to bright probe flashes in the main experiment, and  
1149 OFF cells were analyzed with dark probe flashes. We determined the spatial  
1150 receptive fields of RGCs by calculating the linear filters for each region (checker)  
1151 defined by the binary checkerboard flickering stimulus. The modulation strength of  
1152 each linear filter, measured as the s.d. along the 500 ms temporal kernel, is an

1153 estimate for how strongly that region drives ganglion cell responses. We fitted the  
1154 resulting 2D-map of s.d. values with a two dimensional Gaussian and took the  $2\text{-}\sigma$   
1155 ellipse (long axis) as the receptive field diameter. For all other figures and analyses,  
1156 we converted spike times to estimates of firing rate by convolving these times with a  
1157 Gaussian of  $\sigma = 10$  ms standard deviation and amplitude  $0.25 \sigma^{-1} e^{1/2}$ .

1158

1159 For each RGC, we used responses to full-field contrast steps to calculate an ON-  
1160 OFF index, a transiency index, and a response latency index. These indices were  
1161 used to characterize the properties of RGCs (Supplementary Fig. 6) that we included  
1162 in our analyses. The ON-OFF index was calculated by dividing the difference  
1163 between ON and OFF step peak response by their sum. The resulting index values  
1164 ranged between -1 (OFF) and +1 (ON) and were then scaled to span between 0  
1165 (OFF) and +1 (ON). The transiency index was defined as the ratio of the response  
1166 area within the first 400 ms and the total response area spanning 2,000 ms. The  
1167 resulting index had a value of 1 for pure transient cells. Response latency was  
1168 calculated as the time from stimulus onset to 90% of peak response. This value was  
1169 normalized to the maximum response latency in our dataset to create the response  
1170 latency index.

1171

1172 To quantify retinal “saccadic suppression”, we first determined a “baseline response”,  
1173 defined as the response to a probe flash approximately 2 s after texture displacement  
1174 onset (delay between 1,967 to 2,100 ms, depending on the specific flash times used  
1175 in a specific experiment). This baseline response was compared to responses of the  
1176 same cell to the same flash when it occurred at an earlier time (i.e. closer in time to  
1177 the “saccade”). Usually, the saccade-like texture displacements themselves caused

1178 significant neural responses even without flashes (“saccade-response”, e.g. Fig. 3b),  
1179 and the responses to the flashes were superimposed on these “saccade-responses”  
1180 (Fig. 3c). We therefore first isolated the component of the responses caused by the  
1181 flashes by subtracting the “saccade-responses” from the composite responses.

1182

1183 To get a robust estimate of the response to “saccades” alone (i.e. without any  
1184 flashes), we averaged spike rate from before “saccade” onset up until the next  
1185 “saccade” onset for conditions in which no flash was presented, or until just before  
1186 the flash onset for conditions in which a “post-saccade” flash was presented. This  
1187 was done for each of the 39 successive “saccades” in a given trial.

1188

1189 We then computed a neural modulation index, ranging from -1 to +1. A value of -1  
1190 represents complete suppression of flash-induced responses, whereas +1 indicates  
1191 “complete enhancement” of flash-induced responses (that is, there was only a  
1192 response to a flash after saccades, but not to a flash in isolation). A modulation index  
1193 of 0 meant no change in flash-induced response relative to the “baseline” response.  
1194 The modulation index of an RGC for a given flash delay  $d$  after “saccade” onset was  
1195 calculated as  $(r_d - r_b)/(r_d + r_b)$  where  $r_d$  is the peak firing rate for the flash-component  
1196 of the response (see above for how we isolated this from the composite  
1197 “saccade”+flash response) and  $r_b$  is the peak firing rate for the baseline flash  
1198 response (i.e. the same flash but occurring ~2 s away from any “saccade”; see  
1199 above). In all cases, peak firing rate was estimated after averaging responses from  
1200 all repetitions of a given condition (delay  $d$  or baseline) for a given RGC. For ON  
1201 cells, the modulation index was based only on responses to bright flashes, and for  
1202 OFF cells, it was based on responses to dark flashes. For some analyses, we also

1203 calculated modulation indices of RGCs for each of the 39 individual “saccades” using  
1204 the same procedure.

1205

1206 In some cells and trials, individual “saccades” from the sequence of 39 were  
1207 discarded. This happened when the baseline response peak was less than 60% of  
1208 the median baseline response peak across the 39 “saccades” of a given trial. We did  
1209 this to ensure that our modulation indices were not marred by a numerator and  
1210 denominator approaching zero (e.g. if both flash and baseline responses were weak).  
1211 We did, however, re-include sequences in which the peak response to the flash after  
1212 the “saccade” was above the median baseline response peak (across the 39  
1213 “saccades”). This was done in order to re-include sequences (if discarded by the first  
1214 step) for which the baseline flash response was weak but a flash after “saccades”  
1215 nonetheless gave a robust response. For example, this could happen if a cell did not  
1216 respond to a flash in isolation but the “saccade” enhanced the response to a flash  
1217 following it. Our main results (e.g. Fig. 3) were highly robust to such scenarios.

1218

1219 Finally, to perform statistics, we applied tests at either the individual cell level or at  
1220 the level of the population. At the individual cell level, we determined whether a given  
1221 RGC’s modulation index for a probe flash presented at a given delay was  
1222 significantly different from 0 (i.e. “Is the response of this cell modulated by the  
1223 ‘saccade’?”). For this, we performed a one-tailed sign test of the null hypothesis that  
1224 the 39 individual modulation indices came from a distribution with zero median  
1225 against the alternative hypothesis that the median was below (for negative  
1226 modulation index) or above (for positive modulation index) zero. The modulation  
1227 index was considered significant (i.e. the flash response was modulated by the  
1228 “saccade”) at  $p < 0.05$  if the test had a power  $(1 - \beta)$  of at least 0.8. At the population

1229 level, we determined whether the retinal output as a whole was modulated by  
1230 “saccades”. For this, we performed a two-tailed Wilcoxon signed rank test of the null  
1231 hypothesis that the median of the distribution of modulation indices did not differ from  
1232 0. Lastly, we tested whether the modulation index of the population was significantly  
1233 different across textures. For this, we performed a two-tailed Wilcoxon signed rank  
1234 test of the null hypothesis that the median of the distribution of modulation indices did  
1235 not differ across textures. Since our modulation index was based on responses to the  
1236 brief probe flashes, it could only be computed for cells that did respond to these flash  
1237 stimuli (mouse: N = 688 of 1,423 recorded cells; pig: N = 228 of 394). Only these  
1238 cells, showing a measurable baseline flash response, were included in our analyses  
1239 for retinal “saccadic suppression” (Fig. 3e, Supplementary Fig. 5).

1240  
1241 To quantify retinal “saccadic suppression” in our control experiments with structure-  
1242 free uniform backgrounds and luminance steps in place of textures and texture  
1243 displacements (Fig. 4d), we used the same analyses and statistical procedures to  
1244 those described above for the texture displacement paradigm. The only difference  
1245 was that instead of 39 successive “saccades” in a trial, we now had either 57 or 157  
1246 successive full-field luminance steps (depending on experiment setting). 22 of 57 or  
1247 66 of 157 steps had a Michelson contrast in the range of +/- 0.03 to 0.15 and these  
1248 steps were used to quantify suppression for low contrast luminance steps. 24 of 57 or  
1249 58 of 157 steps had a Michelson contrast in the range of +/- 0.20 to 0.40 and were  
1250 used to quantify suppression for high contrast luminance steps. From the perspective  
1251 of visual transients across the retina, low contrast luminance steps are equivalent to  
1252 fine texture displacements over receptive fields, and high contrast luminance steps  
1253 are equivalent to coarse texture displacements. This is simply because of the spatial  
1254 relationship between receptive field sizes and texture spatial scales: a fine texture

1255 presents both dark and bright blobs within individual receptive fields both before and  
1256 after the texture displacement (resulting in a low contrast change in luminance over  
1257 the receptive fields); on the other hand, a coarse texture has dark or bright blobs that  
1258 are of similar size to the receptive fields (resulting in the potential for a very large  
1259 contrast change in luminance over the receptive fields after the texture  
1260 displacement). As shown in Fig. 4d, low and high contrast luminance steps resulted  
1261 in the modulation of ganglion cell responses to the probe flashes that was  
1262 reminiscent of the modulation observed after displacement of fine and coarse  
1263 textures, respectively (also validated perceptually in Fig. 5). Similar to the texture  
1264 displacement paradigm, the modulation index was based on responses to brief probe  
1265 flashes, and it could therefore only be computed for cells that did respond to these  
1266 flash stimuli (N = 376 of 650 recorded RGCs in mouse). The modulation index for ON  
1267 RGCs was calculated from responses to bright probe flashes, and that for OFF  
1268 RGCs was calculated from responses to dark flashes.

1269

#### 1270 *Human psychophysics data analysis and statistics*

1271 We analyzed eye movements in all trials. We detected saccades using established  
1272 methods<sup>41,76</sup>, and we manually inspected all trials to correct for mis-detections. In  
1273 experiments requiring a saccade (e.g. Fig. 1), we excluded from analysis any trials  
1274 with premature (before saccade instruction) or late (>500 ms reaction time)  
1275 saccades. We also rejected all trials in which saccades landed >0.5 deg from the  
1276 saccade target. In experiments requiring fixation, we excluded from analysis any  
1277 trials in which a saccade or microsaccade happened anywhere in the interval from  
1278 200 ms before to 50 ms after any flash or grating onset.

1279

1280 For experiments with saccades (e.g. Fig. 1), we obtained time courses of perception  
1281 by calculating, for each trial, the time of flash or grating onset from saccade onset.  
1282 We then binned these times into 50 ms bins that were moved in 5 ms bin-steps  
1283 relative to saccade onset. Within each bin, we calculated the proportion of correct  
1284 trials, and we obtained full time courses of this perceptual measure. We obtained  
1285 time course curves for each subject individually, and we then averaged the curves for  
1286 the individual subjects in summary figures. All of our analyses were robust at the  
1287 individual subject level as well (e.g. Supplementary Fig. 2).

1288

1289 For experiments with simulated saccades (i.e. saccade-like texture displacements),  
1290 or background luminance steps (Fig. 5), there were discrete flash or grating times  
1291 relative to “simulated saccade” onset, so no temporal binning was needed. At each  
1292 flash or grating time, we simply calculated the proportion of correct trials.

1293

1294 When we fitted performance to psychometric curves (e.g. Supplementary Fig. 3a, b),  
1295 we used *the psignifit 4 toolbox*<sup>77</sup>, and we used an underlying beta-binomial model. In  
1296 all psychometric curve fits, we also included lapse parameters among the fitted  
1297 parameters, in order to account for potential small deviations from either perfect  
1298 ceiling performance or perfect floor (chance) performance at the extremes of the  
1299 psychometric curves.

1300

1301 We also used the same toolbox to analyze the variants of Human Experiments 1 and  
1302 2 in which we collected full psychometric curves (Figs. 2, 7). For these experiments,  
1303 we defined the threshold of an individual subject as the flash luminance level that  
1304 resulted in correct perceptual performance at a value of 62.5% of the total dynamic  
1305 range of the subject’s psychometric curve (that is, 62.5% of the dynamic range of the

1306 fitted psychometric curve after the inclusion of lapse rates). We then plotted the value  
1307 of such threshold as a function of flash time relative to real or simulated saccade  
1308 time.

1309

1310 For some analyses of Human Experiment 3 and its control version, we calculated a  
1311 “suppression ratio” as a visualization aid (e.g. Fig. 8). This was obtained as follows.  
1312 For a given spatial frequency grating, we calculated the fraction of correct trials within  
1313 a given time window (from either simulated or real saccade onset) divided by the  
1314 fraction of correct trials for the same spatial frequency when there was neither a  
1315 saccade nor a virtual monitor and texture displacement (i.e. baseline perception of a  
1316 given spatial frequency). This ratio therefore revealed the effect of suppression  
1317 independently from the underlying visibility of any given spatial frequency<sup>7</sup>. However,  
1318 note that we also report raw proportions of correct trials in all conditions.

1319

1320 All error bars that we show denote s.e.m. across individual subjects, except where  
1321 we report individual subject analyses and control analyses. For individual subject  
1322 performance, error bars denote s.e.m. across trials; for control analyses, error bars  
1323 denote 95% confidence intervals (e.g. Supplementary Fig. 3a, b) or s.d. (e.g.  
1324 Supplementary Fig. 3d, f). All error bar definitions are specified in the corresponding  
1325 figures and/or legends.

1326

1327 To statistically validate if the time courses for perceptual localization performance for  
1328 saccades across the different background textures (coarse versus fine) differed  
1329 significantly from each other (e.g. Fig. 1), we used a random permutation test with  
1330 correction for time clusters of adjoining significant p-values<sup>39,40</sup>. First, for each time  
1331 bin, we calculated a test statistic comparing performance for coarse versus fine

1332 background textures. This test statistic was the difference between the proportion of  
1333 correct responses for the different textures. Then, we performed a random  
1334 permutation with 1,000 repetitions for each time bin; that is, we collected all trials of  
1335 both conditions, within a given time bin, into a single large set, and we randomly  
1336 assigned measurements as coming from either coarse or fine textures, while at the  
1337 same time maintaining the relative numbers of observations per time bin for each  
1338 texture condition. From this resampled data, we calculated the test statistic again,  
1339 and we repeated this procedure 1,000 times. Second, we checked, for each time bin,  
1340 whether our original test statistic was bigger than 95% of the resampled test statistics  
1341 (i.e. significant), and we counted the number of adjoining time bins that were  
1342 significant at this level (i.e. clusters of time bins in which there was a difference  
1343 between coarse and fine textures). We then repeated this for all 1,000 resampled test  
1344 statistics. The p-value for our original clusters was then calculated as the number of  
1345 resampled clusters that were bigger or the same size as the original clusters, divided  
1346 by the total number of repetitions (1,000). This procedure was described in detail  
1347 elsewhere<sup>40</sup>. We followed a conservative approach, paying no attention to which bins  
1348 in the resampled data formed a cluster of time bins. As discussed elsewhere<sup>40</sup>, our  
1349 statistical analysis constituted a highly conservative approach to establishing  
1350 significance of differences between time courses for coarse and fine textures. In  
1351 Human Experiment 3, we used the same approach to compare time courses of  
1352 suppression ratio for coarse and fine surround contexts with real saccades.

1353  
1354 For Human Experiment 2, we had discrete flash times relative to texture  
1355 displacement onset. Here, the comparison between coarse and fine textures was  
1356 tested with a Bonferroni-corrected  $\chi^2$  test at corresponding flash times. To compare  
1357 between real and simulated saccades in Human Experiments 1 and 2, we also ran a

1358 Bonferroni-corrected  $\chi^2$  test. We only considered time bins in the real saccade data  
1359 that corresponded to the discrete flash times in the simulated saccade data. A  
1360 Bonferroni correction was necessary because we tested the same data sets on  
1361 multiple time bins with the same hypothesis (that there is a difference in time  
1362 courses).

1363

1364 In Human Experiment 3, we also compared suppression ratios for real and simulated  
1365 saccades for a given texture surround. We again used a Bonferroni-corrected  $\chi^2$  test.  
1366 This was justified because within a given surround, baseline data were the same for  
1367 real and simulated saccades. Therefore, the relationship between the proportion of  
1368 correct localizations and suppression ratio was identical. In contrast, testing  
1369 suppression ratios between fine and coarse surrounds in the same experiment with a  
1370  $\chi^2$  test was not applicable because baseline values differed. Therefore, we used  
1371 instead a random permutation test with 5,000 repetitions. To compare the different  
1372 spatial frequency Gabor gratings in one bin or time stamp, we used the Kruskal-  
1373 Wallis test.

1374

1375 For the psychometric versions of Human Experiment 3 (Figs. 9, 10), we used similar  
1376 analyses on perceptual thresholds to those used in the psychometric versions of  
1377 Human Experiments 1 and 2 (Figs. 2, 7).

1378

#### 1379 *Data availability*

1380 All data presented in this paper are stored and archived on secure institute  
1381 computers and are available upon reasonable request.

1382 **Acknowledgements**

1383 Andreas Hierlemann provided the HiDens CMOS MEA system and helped establish  
1384 our high-density MEA recordings. Roland Diggelmann helped in setting up the  
1385 pipeline (including providing code) for automatic spike sorting of high-density MEA  
1386 recordings. This work was supported by funds of the Deutsche  
1387 Forschungsgemeinschaft (DFG) to the Werner Reichardt Center for Integrative  
1388 Neuroscience (EXC 307) and to T.A.M. (MU3792/3-1). T.A.M. received support from  
1389 the Tistou and Charlotte Kerstan Foundation. T.A.M. and Z.M.H. were also supported  
1390 by an intra-mural funding program (Projekt 2013-05) of the Werner Reichardt Centre  
1391 for Integrative Neuroscience. F.F. was supported by a Swiss National Science  
1392 Foundation Ambizione grant (PZ00P3\_167989).

1393

1394 **Author contributions**

1395 S.I., M.B., T.A.M., Z.M.H. designed the overall study; S.I., M.B., T.A.M., Z.M.H.  
1396 designed experiments; S.I. performed *ex vivo* retina experiments; M.B., Z.M.H.  
1397 performed human psychophysics experiments; S.I., M.B., F.F., T.A.M., Z.M.H.  
1398 analyzed data; S.I., M.B., F.F., T.A.M., Z.M.H. wrote manuscript.

1399

1400 **Competing interests**

1401 The authors declare no competing interests.

1402 **References**

- 1403 1. O'Regan, J. K. & Noë, A. A sensorimotor account of vision and visual  
1404 consciousness. *Behav. Brain Sci.* **24**, 939–973 (2001).
- 1405 2. Wurtz, R. H. Neuronal mechanisms of visual stability. *Vision Res.* **48**, 2070–89  
1406 (2008).
- 1407 3. Wurtz, R. H., Joiner, W. M. & Berman, R. A. Neuronal mechanisms for visual  
1408 stability: Progress and problems. *Philos. Trans. R. Soc. B Biol. Sci.* **366**, 492–  
1409 503 (2011).
- 1410 4. Thiele, A., Henning, P., Kubischik, M. & Hoffmann, K. P. Neural mechanisms of  
1411 saccadic suppression. *Science (80-. )*. **295**, 2460–2462 (2002).
- 1412 5. Zuber, B. L. & Stark, L. Saccadic suppression: Elevation of visual threshold  
1413 associated with saccadic eye movements. *Exp. Neurol.* **16**, 65–79 (1966).
- 1414 6. Beeler, G. W. Visual threshold changes resulting from spontaneous saccadic  
1415 eye movements. *Vision Res.* **7**, 769–775 (1967).
- 1416 7. Chen, C.-Y. & Hafeed, Z. M. A neural locus for spatial-frequency specific  
1417 saccadic suppression in visual-motor neurons of the primate superior  
1418 colliculus. *J. Neurophysiol.* **117**, 1657–1673 (2017).
- 1419 8. Martin, E. Saccadic suppression: a review and an analysis. *Psychol. Bull.* **81**,  
1420 899–917 (1974).
- 1421 9. Riggs, L. A. & Manning, K. A. Saccadic suppression under conditions of  
1422 whiteout. *Invest. Ophthalmol. Vis. Sci.* **23**, 138–143 (1982).
- 1423 10. Volkman, F. C. Human visual suppression. *Vision Res.* **26**, 1401–1416  
1424 (1986).
- 1425 11. Burr, D. C., Morrone, M. C. & Ross, J. Selective suppression of the  
1426 magnocellular visual pathway during saccadic eye movements. *Nature* **371**,  
1427 511–513 (1994).
- 1428 12. Ross, J., Burr, D. C. & Morrone, M. C. Suppression of the magnocellular  
1429 pathway during saccades. *Behav. Brain Res.* **80**, 1–8 (1996).
- 1430 13. Bremmer, F., Kubischik, M., Hoffmann, K.-P. & Krekelberg, B. Neural dynamics  
1431 of saccadic suppression. *J. Neurosci.* **29**, 12374–12383 (2009).
- 1432 14. Hafeed, Z. M. & Krauzlis, R. J. Microsaccadic suppression of visual bursts in the  
1433 primate superior colliculus. *J. Neurosci.* **30**, 9542–9547 (2010).
- 1434 15. Krekelberg, B. Saccadic suppression. *Curr. Biol.* **20**, R228–R229 (2010).
- 1435 16. Duffy, F. H. & Lombroso, C. T. Electrophysiological evidence for visual

- 1436 suppression prior to the onset of a voluntary saccadic eye movement. *Nature*  
1437 **218**, 1074–1075 (1968).
- 1438 17. Diamond, M. R., Ross, J. & Morrone, M. C. Extraretinal control of saccadic  
1439 suppression. *J. Neurosci.* **20**, 3449–3455 (2000).
- 1440 18. Ross, J., Morrone, M. C., Goldberg, M. E. & Burr, D. C. Changes in visual  
1441 perception at the time of saccades. *Trends Neurosci.* **24**, 113–121 (2001).
- 1442 19. Gremmler, S. & Lappe, M. Saccadic suppression during voluntary versus  
1443 reactive saccades. *J. Vis.* **17**, 1–10 (2017).
- 1444 20. Mackay, D. M. Elevation of visual threshold by displacement of retinal image.  
1445 *Nature* **225**, 90–92 (1970).
- 1446 21. García-Pérez, M. A. & Peli, E. Visual contrast processing is largely unaltered  
1447 during saccades. *Front. Psychol.* **2**, 1–15 (2011).
- 1448 22. Ilg, U. J. & Hoffmann, K. P. Motion perception during saccades. *Vision Res.* **33**,  
1449 211–220 (1993).
- 1450 23. Campbell, F. W. & Wurtz, R. H. Saccadic omission: Why we do not see a grey-  
1451 out during a saccadic eye movement. *Vision Res.* **18**, 1297–1303 (1978).
- 1452 24. Mitrani, L., Mateeff, S. & Yakimoff, N. Is saccadic suppression really saccadic?  
1453 *Vision Res.* **11**, 1157–1161 (1971).
- 1454 25. Matin, E., Clymer, A. B. & Matin, L. Metacontrast and saccadic suppression.  
1455 *Science* **178**, 179–182 (1972).
- 1456 26. Mitrani, L., Yakimoff, N. & Mateeff, S. Saccadic suppression in the presence of  
1457 structured background. *Vision Res.* **13**, 517–521 (1973).
- 1458 27. Mateeff, S., Yakimoff, N. & Mitrani, L. Some characteristics of the visual  
1459 masking by moving contours. *Vision Res.* **16**, 489–492 (1976).
- 1460 28. Brooks, B. A., Impelman, D. M. K. & Lum, J. T. Backward and forward masking  
1461 associated with saccadic eye movement. *Percept. Psychophys.* **30**, 62–70  
1462 (1981).
- 1463 29. Macknik, S. L. & Livingstone, M. S. Neuronal correlates of visibility and  
1464 invisibility in the primate visual system. *Nat. Neurosci.* **1**, 144–149 (1998).
- 1465 30. Castet, E., Jeanjean, S. & Masson, G. S. ‘Saccadic suppression’ – no need for  
1466 an active extra-retinal mechanism. *Trends Neurosci.* **24**, 316–317 (2001).
- 1467 31. Castet, E. Perception of intra-saccadic motion. in *Dynamics of visual motion*  
1468 *processing* 141–160 (Springer US, 2010). doi:10.1007/978-1-4419-0781-3
- 1469 32. Krueger, J. & Fischer, B. Strong periphery effect in cat retinal ganglion cells.

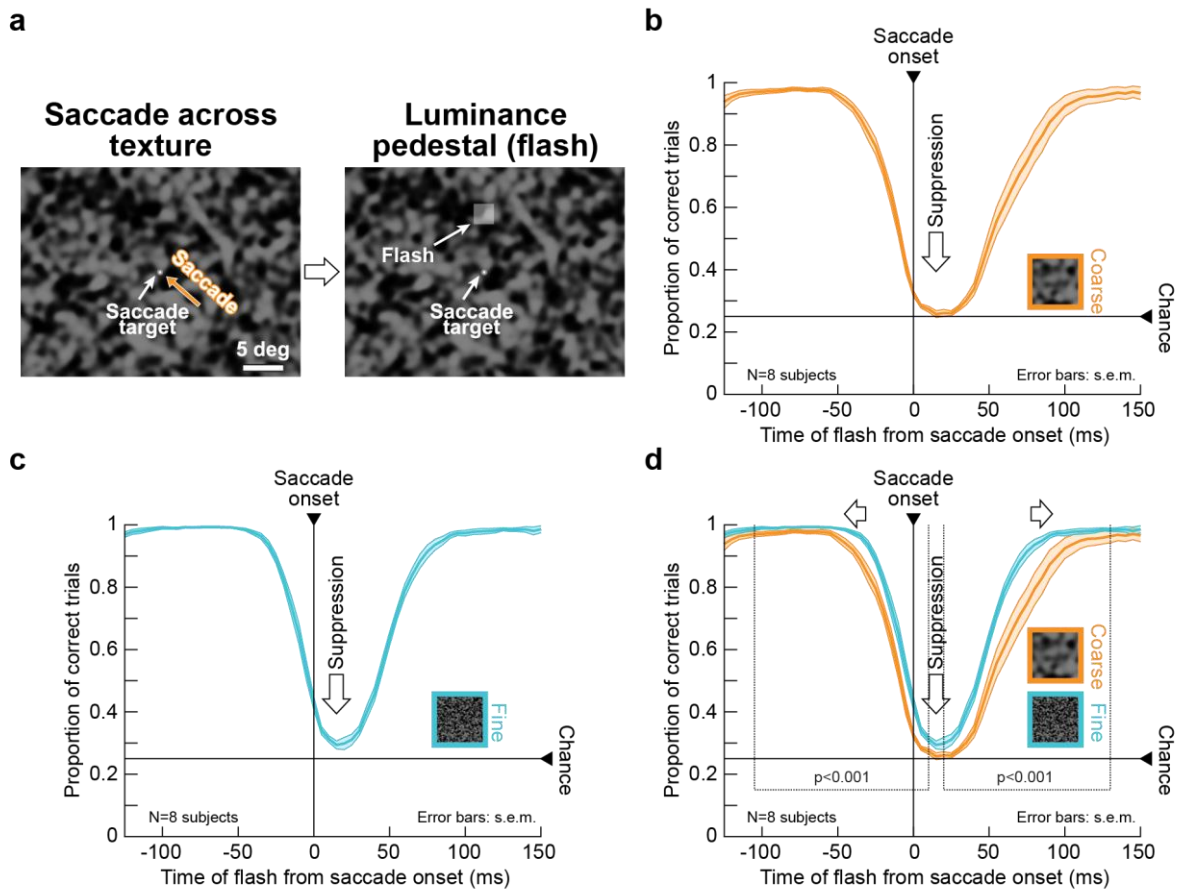
- 1470            Excitatory responses in ON- and OFF-center neurones to single grid  
1471            displacements. *Exp. Brain Res.* **18**, 316–318 (1973).
- 1472    33.    Noda, H. & Adey, W. R. Retinal ganglion cells of the cat transfer information on  
1473            saccadic eye movement and quick target motion. *Brain Res.* **70**, 340–345  
1474            (1974).
- 1475    34.    Barlow, H. B., Derrington, A. M., Harris, L. R. & Lennie, P. The effects of  
1476            remote retinal stimulation on the responses of cat retinal ganglion cells. *J.*  
1477            *Physiol.* **269**, 177–194 (1977).
- 1478    35.    Enroth-Cugell, C. & Jakiela, H. G. Suppression of cat retinal ganglion cell  
1479            responses by moving patterns. *J. Physiol.* **302**, 49–72 (1980).
- 1480    36.    Roska, B. & Werblin, F. Rapid global shifts in natural scenes block spiking in  
1481            specific ganglion cell types. *Nat. Neurosci.* **6**, 600–608 (2003).
- 1482    37.    Passaglia, C. L., Freeman, D. K. & Troy, J. B. Effects of remote stimulation on  
1483            the modulated activity of cat retinal ganglion cells. *J. Neurosci.* **29**, 2467–2476  
1484            (2009).
- 1485    38.    Dacey, D. M. & Petersen, M. R. Dendritic field size and morphology of midget  
1486            and parasol ganglion cells of the human retina. *Proc. Natl. Acad. Sci.* **89**,  
1487            9666–9670 (1992).
- 1488    39.    Maris, E. & Oostenveld, R. Nonparametric statistical testing of EEG- and MEG-  
1489            data. *J. Neurosci. Methods* **164**, 177–190 (2007).
- 1490    40.    Bellet, J., Chen, C.-Y. & Hafed, Z. M. Sequential hemifield gating of  $\alpha$ - and  $\beta$ -  
1491            behavioral performance oscillations after microsaccades. *J. Neurophysiol.* **118**,  
1492            2789–2805 (2017).
- 1493    41.    Chen, C.-Y. & Hafed, Z. M. Postmicrosaccadic Enhancement of Slow Eye  
1494            Movements. *J. Neurosci.* **33**, 5375–5386 (2013).
- 1495    42.    Watson, A. B. & Pelli, D. G. Quest: A Bayesian adaptive psychometric method.  
1496            *Percept. Psychophys.* **33**, 113–120 (1983).
- 1497    43.    Robinson, D. L. & Wurtz, R. H. Use of an extraretinal signal by monkey  
1498            superior colliculus neurons to distinguish real from self-induced stimulus  
1499            movement. *J. Neurophysiol.* **39**, 852–870 (1976).
- 1500    44.    Mayo, J. P. & Sommer, M. A. Neuronal Adaptation Caused by Sequential  
1501            Visual Stimulation in the Frontal Eye Field. *J. Neurophysiol.* **100**, 1923–1935  
1502            (2008).
- 1503    45.    Krock, R. M. & Moore, T. Visual sensitivity of frontal eye field neurons during  
1504            the preparation of saccadic eye movements. *J. Neurophysiol.* **116**, 2882–2891  
1505            (2016).

- 1506 46. Chen, C.-Y., Ignashchenkova, A., Thier, P. & Hafed, Z. M. Neuronal response  
1507 gain enhancement prior to microsaccades. *Curr. Biol.* **25**, 2065–2074 (2015).
- 1508 47. Breitmeyer, B. G. Visual masking: past accomplishments, present status, future  
1509 developments. *Adv. Cogn. Psychol.* **3**, 9–20 (2007).
- 1510 48. Castet, E. & Masson, G. S. Motion perception during saccadic eye movements.  
1511 *Nat. Neurosci.* **3**, 177–83 (2000).
- 1512 49. Ramcharan, E. J., Gnadt, J. W. & Sherman, S. M. The effects of saccadic eye  
1513 movements on the activity of geniculate relay neurons in the monkey. *Vis.*  
1514 *Neurosci.* **18**, 253–258 (2001).
- 1515 50. Reppas, J. B., Usrey, W. M. & Reid, R. C. Saccadic eye movements modulate  
1516 visual responses in the lateral geniculate nucleus. *Neuron* **35**, 961–974 (2002).
- 1517 51. Kleiser, R., Seitz, R. J. & Krekelberg, B. Neural correlates of saccadic  
1518 suppression in humans. *Curr. Biol.* **14**, 386–390 (2004).
- 1519 52. Royal, D. W., Sáry, G., Schall, J. D. & Casagrande, V. A. Correlates of motor  
1520 planning and postsaccadic fixation in the macaque monkey lateral geniculate  
1521 nucleus. *Exp. Brain Res.* **168**, 62–75 (2006).
- 1522 53. Hass, C. A. & Horwitz, G. D. Effects of microsaccades on contrast detection  
1523 and V1 responses in macaques. *J. Vis.* **11**, 3–3 (2011).
- 1524 54. Phongphanphane, P. *et al.* Distinct local circuit properties of the superficial  
1525 and intermediate layers of the rodent superior colliculus. *Eur. J. Neurosci.* **40**,  
1526 2329–2343 (2014).
- 1527 55. Rajkai, C. *et al.* Transient cortical excitation at the onset of visual fixation.  
1528 *Cereb. Cortex* **18**, 200–209 (2008).
- 1529 56. Ibbotson, M. R., Crowder, N. A., Cloherty, S. L., Price, N. S. C. & Mustari, M. J.  
1530 Saccadic modulation of neural responses: possible roles in saccadic  
1531 suppression, enhancement, and time compression. *J. Neurosci.* **28**, 10952–60  
1532 (2008).
- 1533 57. Cloherty, S. L., Mustari, M. J., Rosa, M. G. P. & Ibbotson, M. R. Effects of  
1534 saccades on visual processing in primate MSTd. *Vision Res.* **50**, 2683–2691  
1535 (2010).
- 1536 58. Ibbotson, M. R. & Cloherty, S. L. Visual perception: saccadic omission--  
1537 suppression or temporal masking? *Curr. Biol.* **19**, R493-6 (2009).
- 1538 59. Duhamel, J. R., Colby, C. L. & Goldberg, M. E. The updating of the  
1539 representation of visual space in parietal cortex by intended eye movements.  
1540 *Science* **255**, 90–2 (1992).
- 1541 60. Sommer, M. A. & Wurtz, R. H. Influence of the thalamus on spatial visual

- 1542 processing in frontal cortex. *Nature* **444**, 374–377 (2006).
- 1543 61. Münch, T. A. *et al.* Approach sensitivity in the retina processed by a  
1544 multifunctional neural circuit. *Nat. Neurosci.* **12**, 1308–1316 (2009).
- 1545 62. Farrow, K. *et al.* Ambient Illumination Toggles a Neuronal Circuit Switch in the  
1546 Retina and Visual Perception at Cone Threshold. *Neuron* **78**, 325–338 (2013).
- 1547 63. Tikidji-Hamburyan, A. *et al.* Retinal output changes qualitatively with every  
1548 change in ambient illuminance. *Nat. Neurosci.* **18**, 66–74 (2015).
- 1549 64. Reinhard, K. *et al.* Step-By-Step Instructions for Retina Recordings with  
1550 Perforated Multi Electrode Arrays. *PLoS One* **9**, e106148 (2014).
- 1551 65. Frey, U., Egert, U., Heer, F., Hafizovic, S. & Hierlemann, A. Microelectronic  
1552 system for high-resolution mapping of extracellular electric fields applied to  
1553 brain slices. *Biosens. Bioelectron.* **24**, 2191–2198 (2009).
- 1554 66. Müller, J. *et al.* High-resolution CMOS MEA platform to study neurons at  
1555 subcellular, cellular, and network levels. *Lab Chip* **15**, 2767–2780 (2015).
- 1556 67. Hafed, Z. M. Alteration of Visual Perception prior to Microsaccades. *Neuron* **77**,  
1557 775–786 (2013).
- 1558 68. Grujic, N., Brehm, N., Gloge, C., Zhuo, W. & Hafed, Z. M. Perisaccadic  
1559 perceptual mislocalization is different for upward saccades. *J. Neurophysiol.*  
1560 **120**, 3198–3216 (2018).
- 1561 69. Schwartz, G. W. *et al.* The spatial structure of a nonlinear receptive field. *Nat.*  
1562 *Neurosci.* **15**, 1572–80 (2012).
- 1563 70. Zhang, Y., Kim, I.-J., Sanes, J. R. & Meister, M. The most numerous ganglion  
1564 cell type of the mouse retina is a selective feature detector. *Proc. Natl. Acad.*  
1565 *Sci.* **109**, E2391–E2398 (2012).
- 1566 71. Sakatani, T. & Isa, T. Quantitative analysis of spontaneous saccade-like rapid  
1567 eye movements in C57BL/6 mice. *Neurosci. Res.* **58**, 324–331 (2007).
- 1568 72. Itokazu, T. *et al.* Streamlined sensory motor communication through cortical  
1569 reciprocal connectivity in a visually guided eye movement task. *Nat. Commun.*  
1570 **9**, 338 (2018).
- 1571 73. Peli, E., Arend, L. E., Young, G. M. & Goldstein, R. B. Contrast sensitivity to  
1572 patch stimuli: effects of spatial bandwidth and temporal presentation. *Spat. Vis.*  
1573 **7**, 1–14 (1993).
- 1574 74. Diggelmann, R., Fiscella, M., Hierlemann, A. & Franke, F. Automatic spike  
1575 sorting for high-density microelectrode arrays. *J. Neurophysiol.* **120**, 3155–  
1576 3171 (2018).

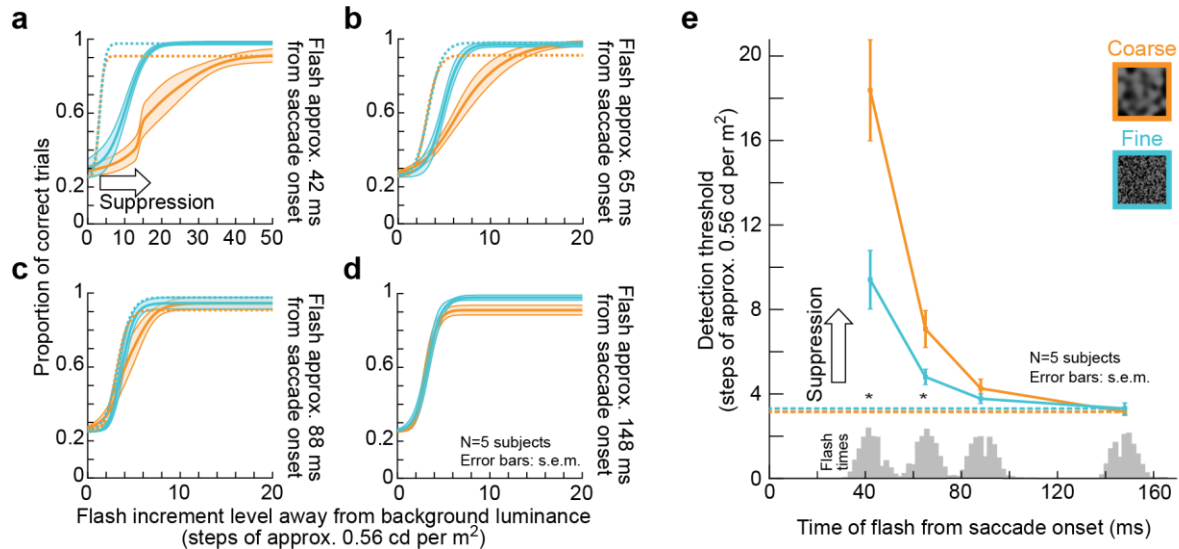
- 1577 75. Idrees, S., Franke, F., Diggelmann, R., Hierlemann, A. & Münch, T. A.  
1578 UnitBrowser - A Tool to Evaluate and Post-Process Units Sorted by Automatic  
1579 Spike Sorting Algorithms. *Front. Neurosci.* **10**, (2016).
- 1580 76. Bellet, M. E., Bellet, J., Nienborg, H., Hafed, Z. M. & Berens, P. Human-level  
1581 saccade detection performance using deep neural networks. *J. Neurophysiol.*  
1582 **121**, 646–661 (2019).
- 1583 77. Schütt, H. H., Harmeling, S., Macke, J. H. & Wichmann, F. A. Painfree and  
1584 accurate Bayesian estimation of psychometric functions for (potentially)  
1585 overdispersed data. *Vision Res.* **122**, 105–123 (2016).
- 1586

1587 **Figures**



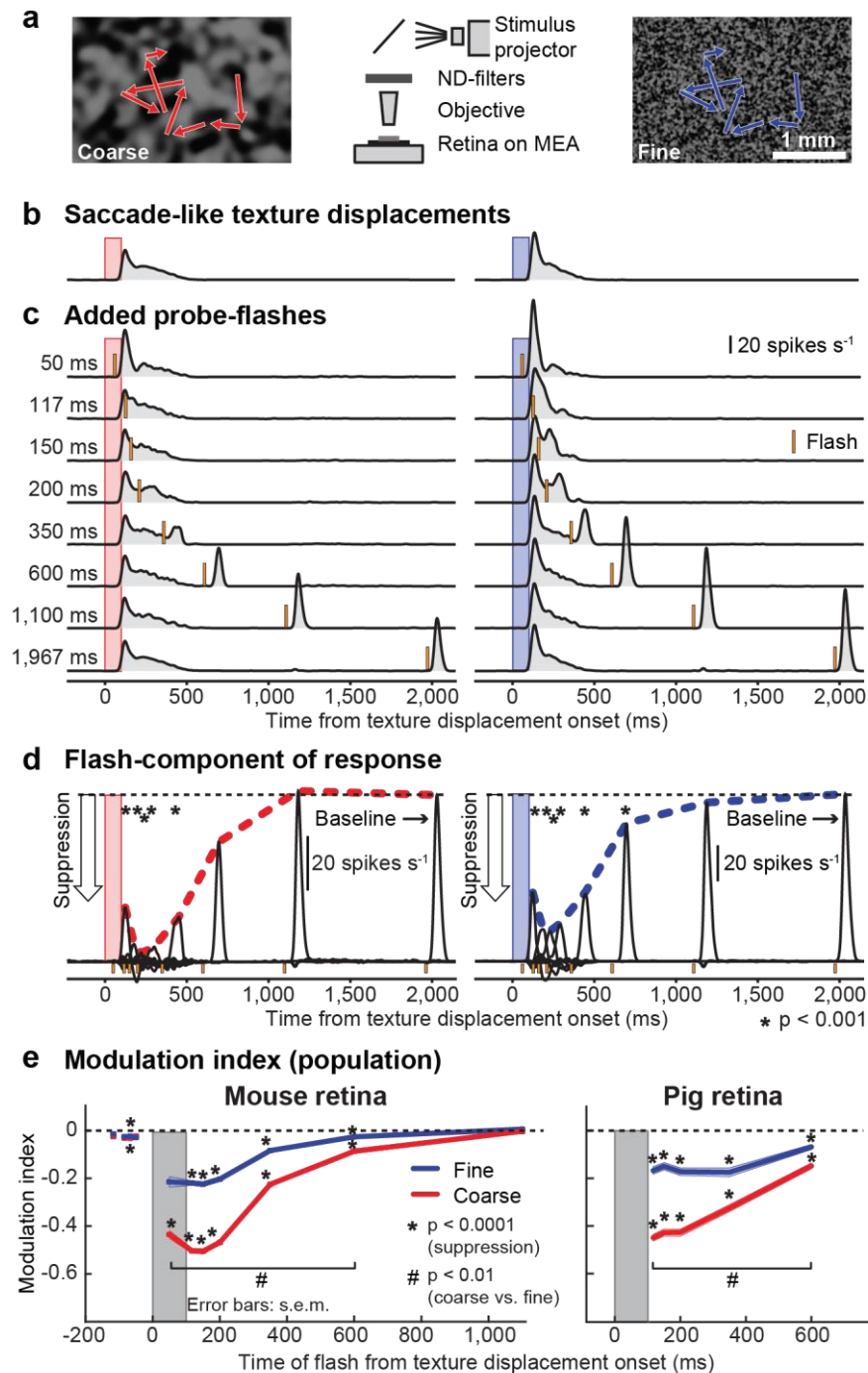
1588  
1589  
1590  
1591  
1592  
1593  
1594  
1595  
1596  
1597  
1598  
1599  
1600  
1601  
1602

**Figure 1 Image dependence of perceptual saccadic suppression.** (a) Human subjects generated saccades from one of four diagonal locations towards display center (here: from the lower right). A luminance pedestal was flashed peri-saccadically at one of four locations around display center (right, left, up, or down; here: up). The example shows the coarse background texture (insets in **c**, **d** show fine textures for comparison; also see Supplementary Fig. 1 and Methods). (b, c) Subjects failed to localize peri-saccadic flashes with both coarse (b) and fine (c) textures (we binned perceptual reports as a function of flash time from saccade onset using 50-ms bins moved in steps of 5 ms). (d) Perceptual suppression started earlier and lasted longer with a coarse background (also see Fig. 2). The highlighted time points denote significantly different ( $p < 0.001$ ) time clusters between the coarse and fine conditions (Methods). Curves show averages ( $\pm$  s.e.m. bounds) of individual subjects' suppression curves. Supplementary Figs. 2, 3 show individual subject results, as well as controls for flash visibility (in the absence of saccades) and saccade motor variability.



1603  
1604  
1605  
1606  
1607  
1608  
1609  
1610  
1611  
1612  
1613  
1614  
1615  
1616  
1617  
1618  
1619  
1620  
1621  
1622  
1623  
1624  
1625  
1626

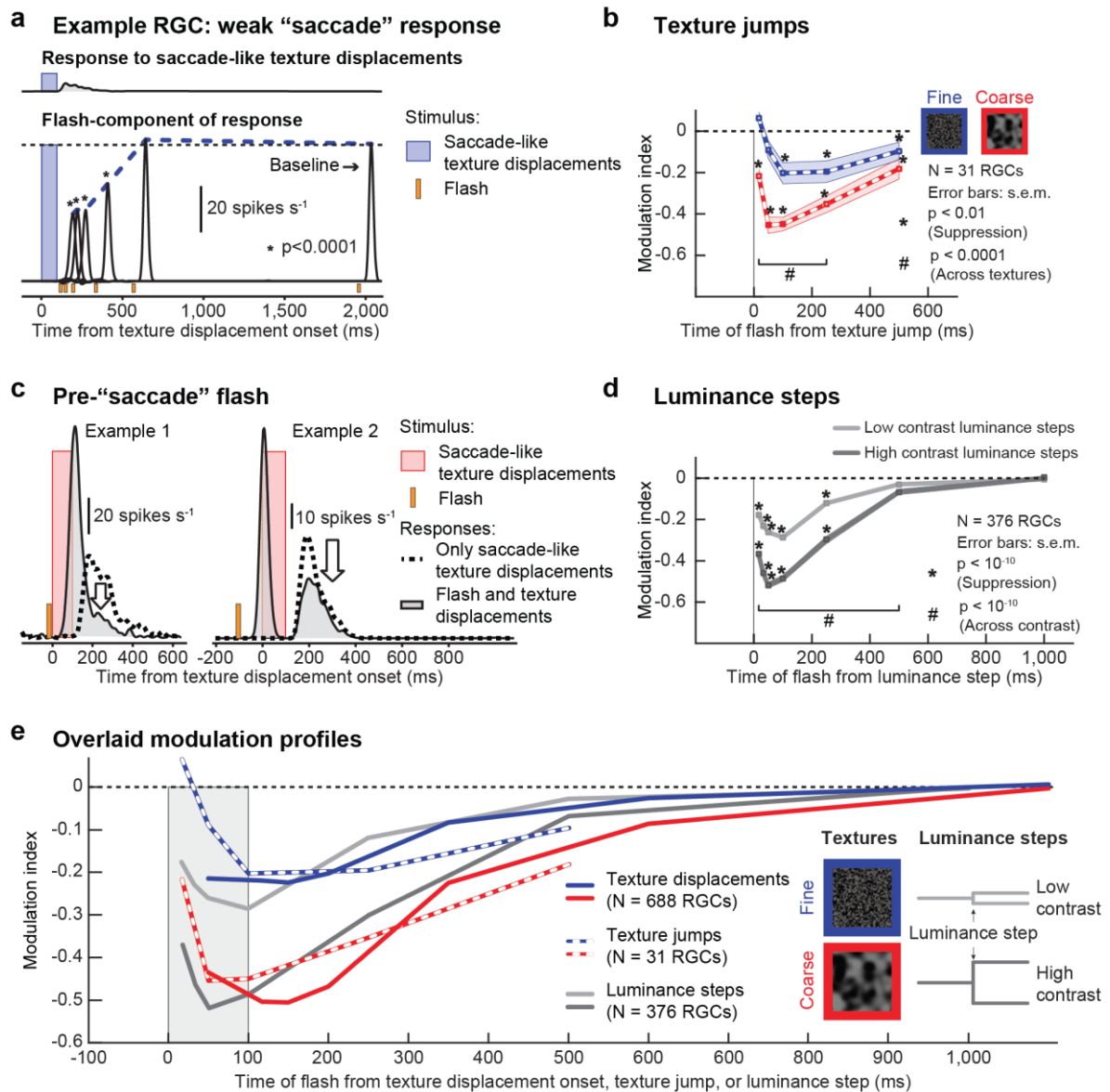
**Figure 2 Image-dependent elevation of perceptual thresholds across saccades. (a-d)** We repeated the experiment of Fig. 1 but collecting full psychometric curves of flash visibility. Solid curves: mean  $\pm$  s.e.m. of the individual psychometric curves of five subjects (see Supplementary Fig. 4 for individual subject results). Dashed curves: psychometric curves near recovery from suppression long after saccades (same data as in **d**). Orange and light-blue indicate data for coarse and fine textures, respectively. **(a)** For flashes approximately 42 ms from saccade onset (Methods), strong perceptual saccadic suppression occurred (compare solid with dashed curves), and the psychometric curve for coarse textures was shifted to higher detection thresholds than that for fine textures, indicating stronger perceptual saccadic suppression. **(b)** At approximately 65 ms after saccade onset, substantial recovery was visible (note the different x-axis scale from **a**), but there was still stronger suppression for coarse than fine textures. **(c, d)** Recovery of visibility continued at later times after saccade onset (88 ms, **c**, and 148 ms, **d**), consistent with Fig. 1. **(e)** Perceptual detection thresholds (i.e. flash luminance levels needed to achieve a certain correct performance rate; Methods) from **a-d** as a function of flash times from saccade onset. Since flash times were determined using online saccade detection (Methods), there was some variability of actual displayed flash times; the gray histograms on the x-axis show the actual distributions of flash times for each group of data from **a-d**. The results confirm the interpretation of Fig. 1: perceptual saccadic suppression was stronger and lasted longer for coarse than for fine background textures. Asterisks denote significant differences between coarse and fine textures (two-sample t-test;  $p < 0.05$ ). The dashed horizontal lines show the detection thresholds at the longest flash times (**d**); note that these thresholds are also similar to those in the visibility control experiments of Supplementary Fig. 3a, b.



1627

1628 **Figure 3 “Saccadic suppression” in retina.** (a) We recorded RGC activity from *ex vivo* retinæ placed  
 1629 on multielectrode arrays (MEA). A coarse (left) or fine (right) texture was repeatedly translated in a  
 1630 saccade-like manner (red or blue scan paths), and we presented brief visual flashes at different times  
 1631 relative to “saccades” (similar to Fig. 1). (b, c) Average activity of an example RGC to 39 texture  
 1632 displacements alone (b) or followed by probe flashes at different time delays (c). Red and blue bars  
 1633 show the timings of the texture displacements; orange bars indicate probe flashes. Flash-induced  
 1634 responses were strongly suppressed immediately following saccade-like texture displacements. (d)  
 1635 Isolated flash responses of the same RGC obtained by subtracting responses in b from those in c.  
 1636 Dashed colored lines highlight the time courses of retinal “saccadic suppression” relative to baseline  
 1637 flash-induced responses. (e) Modulation index highlighting retinal “saccadic suppression” (Methods;  
 1638 negative values indicate suppressed flash-induced neural responses). Both mouse and pig retinæ  
 1639 showed strong suppression during and after texture displacements, which also depended on texture  
 1640 statistics (similar to perception; Figs. 1, 2). Error bars denote s.e.m., and asterisks/hashtags indicate

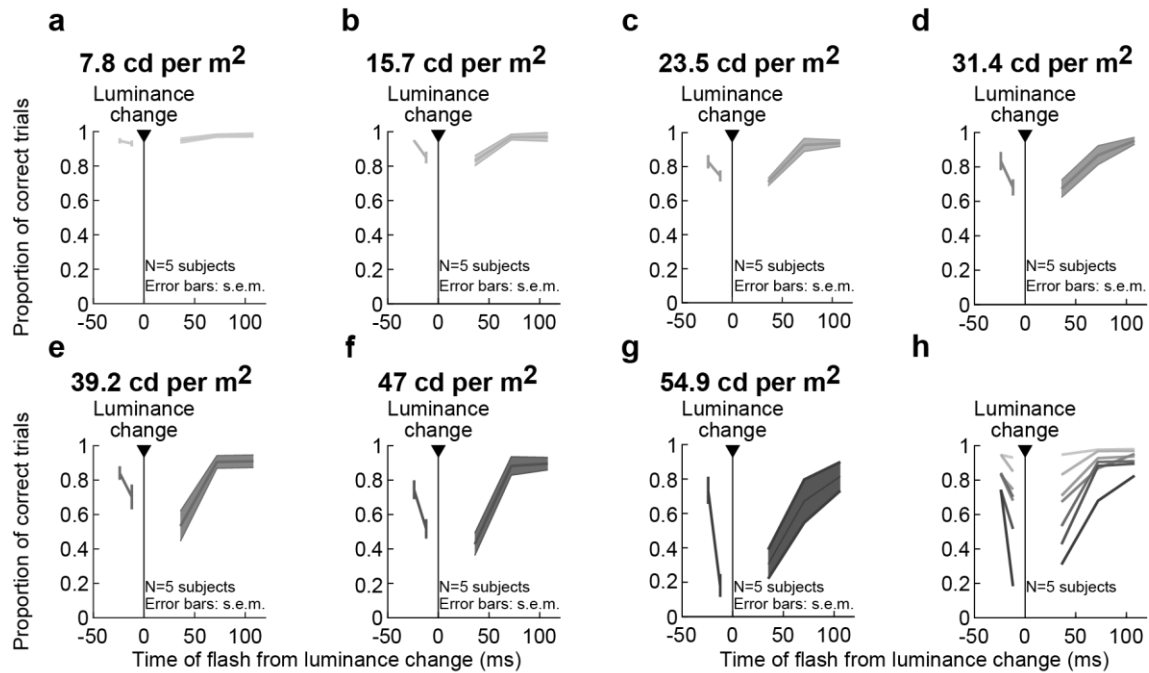
1641 statistical significance (Methods). The numbers of recorded cells at each flash time in **e** were as follows.  
1642 Mouse RGCs: N=179 (-177 ms, -84 ms, -50 ms), 161 (-67 ms), 136 (50 ms), 527 (117 ms), 520 (150  
1643 ms), 502 (200 ms, 600 ms), 688 (350 ms), 345 (1,100 ms); pig RGCs: N=228 for each time point. Figure  
1644 4 shows additional properties of retinal “saccadic suppression”, and Supplementary Figs. 5, 6 show the  
1645 population data underlying panel **e** and different RGC types. Scale bars are defined in their respective  
1646 panels.  
1647



1648

1649 **Figure 4 Stimulus-stimulus interactions in retinal "saccadic suppression".** (a) Example RGC  
 1650 responding only weakly to texture displacements (top), but nevertheless exhibiting strong suppression  
 1651 of flash-induced neural responses (bottom; curves are plotted at the same scale). Suppression was  
 1652 much stronger than the response amplitude to the texture displacements alone. (b) Population  
 1653 modulation index (mean +/- s.e.m.) for a paradigm in which the textures jumped from their start to end  
 1654 positions instantaneously. Strong suppression (\* p < 0.01, two-tailed Wilcoxon signed-rank test) and  
 1655 significant differences between coarse (red) and fine textures (blue; # p < 0.0001, Wilcoxon signed-rank  
 1656 test) were preserved. (c) Two example RGCs showing that a flash presented before saccade-like texture  
 1657 displacements suppressed the response to the displacements, supporting the notion that stimulus-  
 1658 stimulus interactions in the forward direction (first stimulus suppresses the response to the second  
 1659 stimulus) are the main drive for retinal "saccadic suppression". (d) Population modulation index (mean  
 1660 +/- s.e.m.) for a paradigm similar to panel b, but with textures replaced by spatially uniform  
 1661 backgrounds of different intensity. This created visual transients in the form of instantaneous  
 1662 luminance steps. Suppression of flash-induced responses was preserved (\* p < 10<sup>-10</sup>, two-tailed  
 1663 Wilcoxon signed-rank test), and differences between low-contrast (light gray) and high-contrast  
 1664 (dark gray) luminance steps (# p < 10<sup>-10</sup>, two-tailed Wilcoxon signed-rank test) resembled the  
 1665 differences between fine and coarse texture jumps in b. (e) Overlaid modulation profiles from  
 1666 saccade-like texture displacements (Fig. 3e), texture jumps (b), and contrast steps (d). Coarse  
 1667 texture displacements, coarse texture jumps, and high contrast luminance steps had similar  
 1668 modulatory effects on probe flash responses; and so did fine texture displacements, fine texture  
 jumps, and low contrast luminance steps.

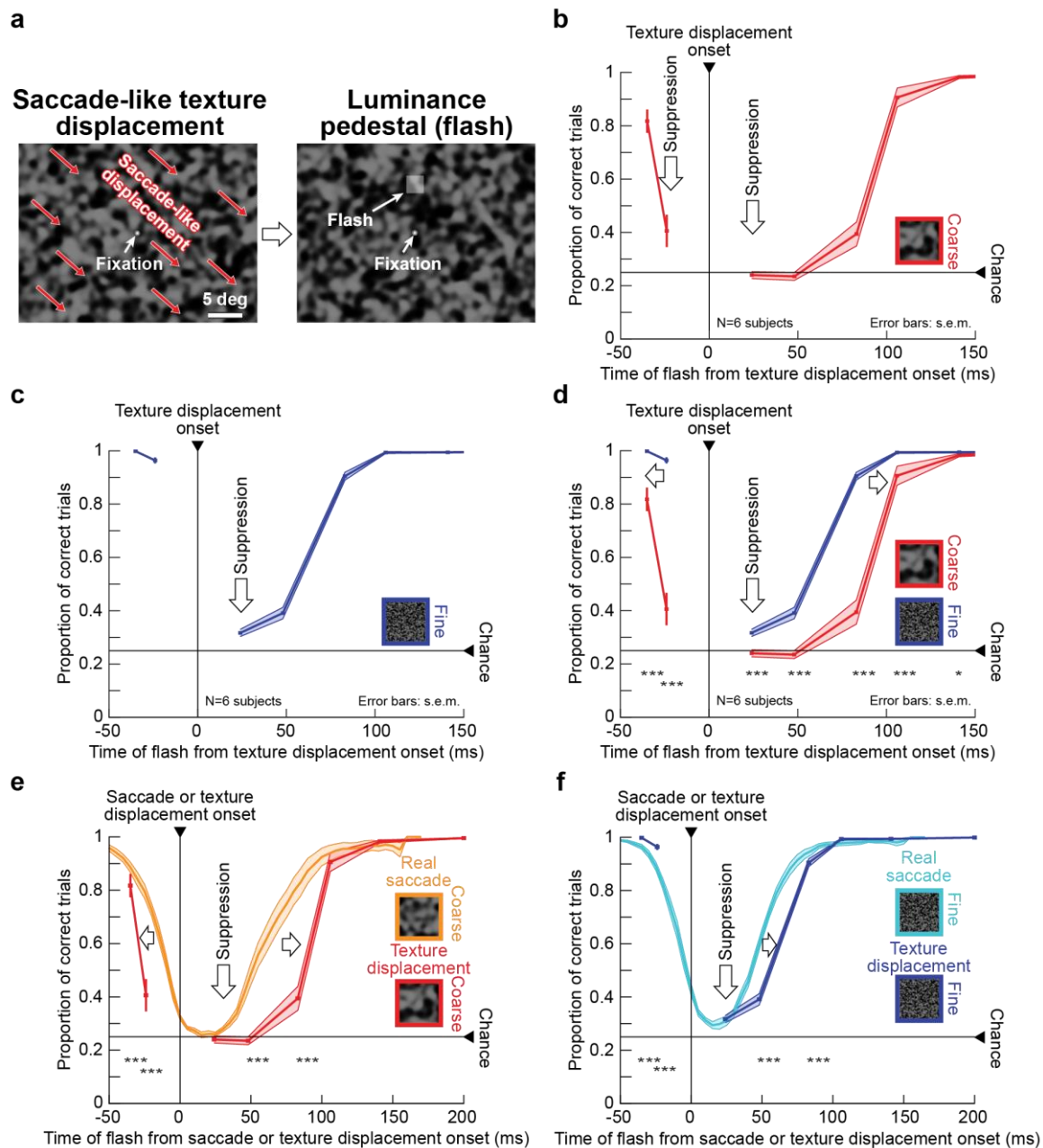
66



1669  
1670  
1671  
1672  
1673  
1674  
1675  
1676  
1677  
1678  
1679  
1680  
1681  
1682

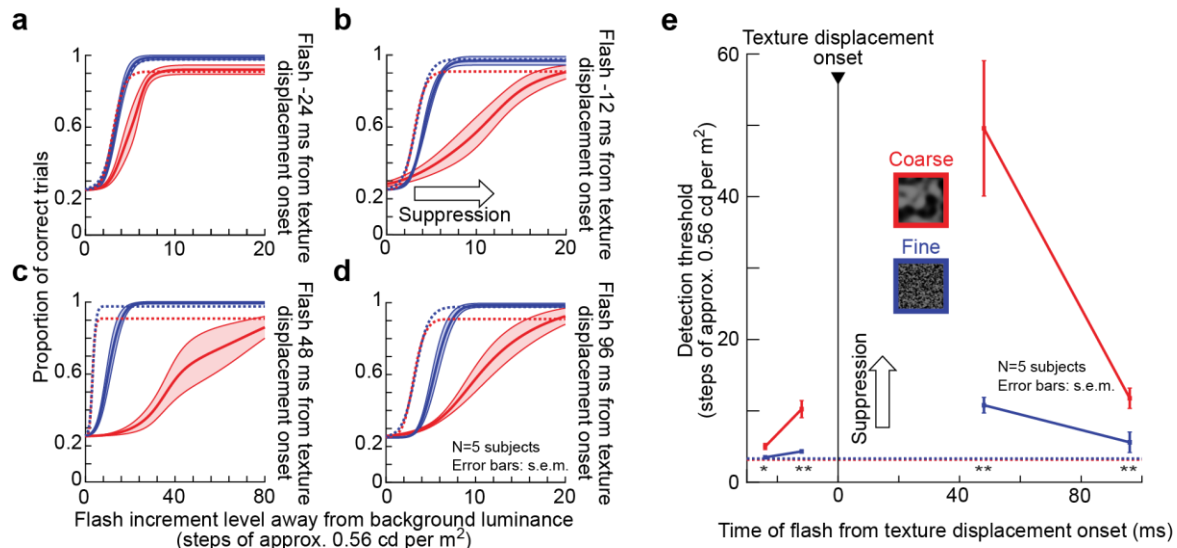
**Figure 5 Stimulus-stimulus interactions in perceptual suppression without saccades** (similar experiment to the retinal paradigm of Fig. 4d). Subjects simply fixated and detected brief flash probes as in the experiments of Figs. 1, 2; here, the flashes happened around the time of a luminance step (i.e. a sudden change in background luminance) instead of a saccade. The title above each panel indicates the absolute value of the luminance change that took place. **(a-g)** Proportion of correct responses as a function of brief flash time from the time of background luminance change. There was progressively stronger perceptual suppression with increasing contrast of the luminance step, consistent with the retinal results of Fig. 4d. **(h)** Summary of panels **a-g**. Darker colors denote larger absolute values of background luminance changes. Since coarse textures (Figs. 1-4) presumably cause larger contrast variations over retinal receptive fields, this suggests that the image dependence of perceptual saccadic suppression (Figs. 1, 2) is mediated by stimulus-stimulus interaction effects originating in the retina (Fig. 4d).

1683



1684  
1685  
1686  
1687  
1688  
1689  
1690  
1691  
1692  
1693  
1694  
1695  
1696  
1697  
1698  
1699  
1700  
1701  
1702

**Figure 6 Image dependence of perceptual suppression without saccades.** (a) Rapid texture displacements simulated saccade-like image displacements, similar to the retina experiments (Fig. 3). We used the same flashes and simulated saccade directions as in Fig. 1. The example shows a coarse texture (fine textures are shown in insets in c, d, and f). (b, c) Pre-, peri-, and post-displacement perceptual suppression occurred for both coarse (b) and fine (c) textures without real saccades. (d) As with real saccades (Fig. 1), suppression started earlier and lasted longer with coarse textures (also compare to similar retinal effects in Fig. 3e). Notably, pre-displacement suppression depended on texture statistics, just like with real saccades (Fig. 1). (e, f) Simulated saccades were associated with significantly longer suppression than real saccades for both fine and coarse textures. For coarse textures (e, which were most effective in causing suppression overall), flashes presented before the “saccade” event were suppressed earlier in the simulated saccade condition than in the real saccade condition (also see Fig. 7); thus, prolonged suppression with texture displacements was not restricted to post-displacement flashes only. Error bars denote s.e.m. across individual subjects’ curves. Asterisks denote significant differences between coarse and fine textures (d) or between real and simulated saccades (e, f) at each indicated time point ( $\chi^2$  tests with Bonferroni corrections; \*  $p < 0.005$  in d and  $p < 0.007$  in e, f; \*\*\*  $p < 0.0001$  in d and  $p < 0.00014$  in e, f). Supplementary Fig. 2 shows individual subject results.

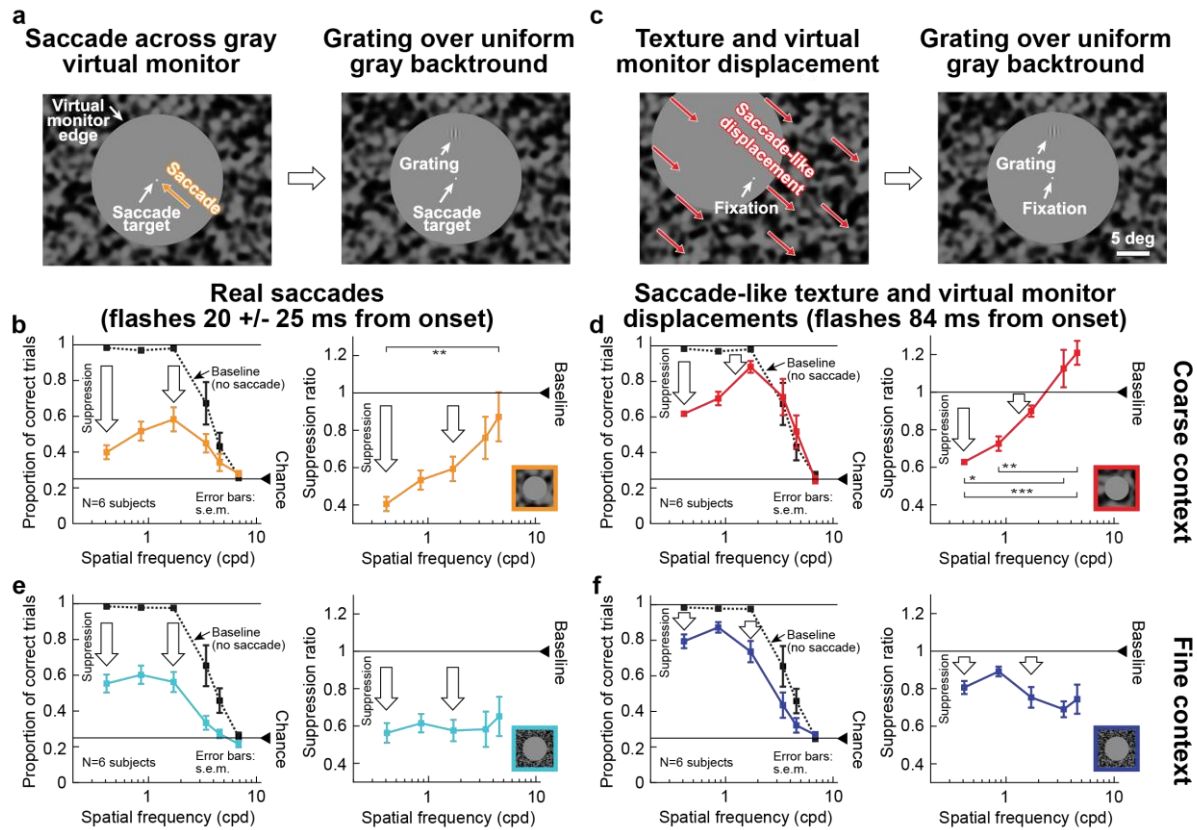


1703  
1704  
1705  
1706  
1707  
1708  
1709  
1710  
1711  
1712  
1713  
1714  
1715  
1716  
1717  
1718  
1719  
1720  
1721  
1722  
1723  
1724  
1725  
1726  
1727

**Figure 7 Image-dependent elevation of perceptual thresholds without saccades.** Similar to Fig. 2, we collected full psychometric curves of flash visibility around the time of simulated saccades (similar paradigm to Fig. 6). **(a-d)** Solid curves: mean  $\pm$  s.e.m of individual psychometric curves of five subjects (see Supplementary Fig. 7 for individual subject results). Dashed curves: baseline data from the same subjects without simulated saccades and long after any real saccades (same data as in Fig. 2d; also similar to Supplementary Fig. 3a, b with additional subjects). Red and blue indicate data for coarse and fine textures, respectively. **(a)** For a flash 24 ms before texture displacement onset, the red curve was shifted rightward towards higher flash contrasts (that is, reduced sensitivity) relative to baseline. This effect was much weaker with fine textures. **(b)** For a flash closer in time to the texture displacement but still before its onset (12 ms before displacement onset), both coarse and fine textures were associated with significant perceptual suppression relative to baseline, consistent with Fig. 6. Moreover, once again, suppression was stronger for coarse than fine textures (evidenced by the larger rightward shift in the psychometric curve). **(c)** Perceptual suppression was the strongest (note the different x-axis scale from the other panels) immediately after texture displacement onset. **(d)** 96 ms after texture displacement onset, there was still significant perceptual suppression, again significantly stronger for coarse than fine textures. This result is consistent with Fig. 6 and highlights the longer-lasting suppression around simulated saccades compared to real saccades (Figs. 1, 2). **(e)** Detection thresholds from **a-d** as a function of flash time from texture displacement onset. Pre- and post-displacement perceptual suppression occurred, and suppression was stronger with coarse textures. Asterisks denote significant differences between coarse and fine textures (two-sample t-test; \*  $p < 0.05$ ; \*\*  $p < 0.01$ ). Horizontal dashed lines show the baseline detection thresholds from Fig. 2d, e. All other conventions are similar to Figs. 1, 2, 6.

1728

1729



1730

1731

1732

1733

1734

1735

1736

1737

1738

1739

1740

1741

1742

1743

1744

1745

1746

1747

1748

1749

1750

1751

1752

1753

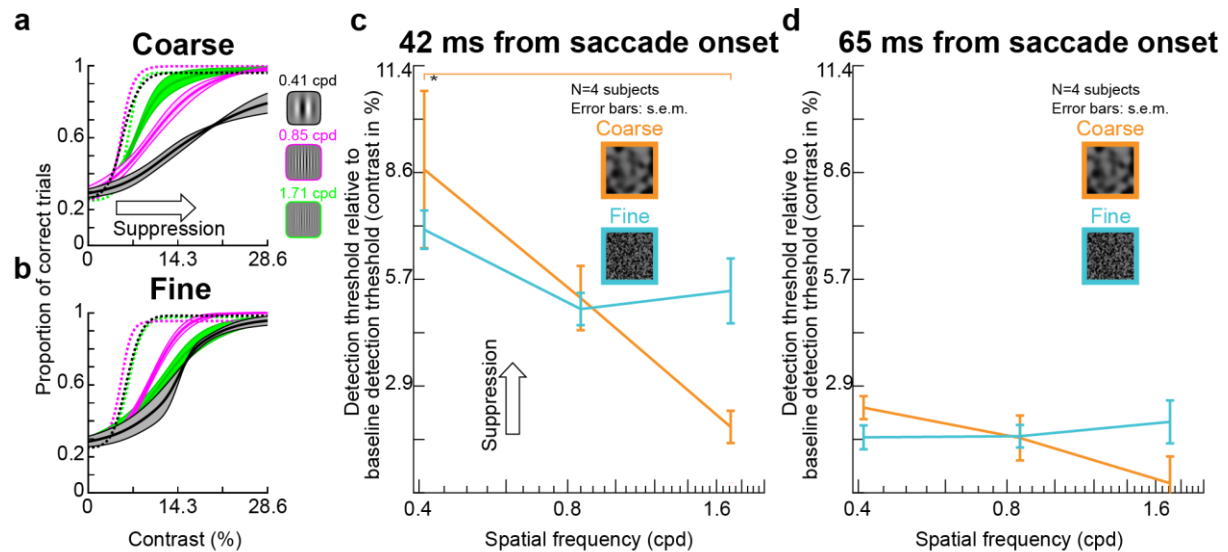
1754

1755

1756

**Figure 8 Selective peri-saccadic suppression of low spatial frequencies<sup>11</sup> is a visual phenomenon.** (a) Left: Subjects made saccades towards display center. Right: gratings were flashed peri-saccadically over a uniform gray background (circular “virtual monitor” surrounded by a coarse texture; saccade directions and flash locations were similar to Figs. 1, 6). (b) Left: proportion of correct localizations of gratings with different spatial frequencies during fixation (“Baseline”; dashed curve) and for peri-saccadic flashes (solid curve). Low spatial frequencies were associated with the strongest suppression relative to baseline. Right: ratio of peri-saccadic to baseline performance (highest spatial frequency not shown because it was at chance performance even in baseline). Suppression depended on grating spatial frequency ( $\chi^2=13.46$ ,  $p=0.0092$ ,  $df=4$ , Kruskal-Wallis test; \*\*  $p<0.01$  for post-hoc pairwise comparisons between the lowest and highest spatial frequencies). (c) Left: we simulated saccade-induced image displacements by translating the virtual monitor and surrounding texture from one corner towards display center. Right: gratings appeared as in a (Methods). (d) The same selective suppression of low spatial frequencies as in b occurred. “Baseline” in this context means both no saccades and no virtual monitor and texture displacements. Suppression depended on spatial frequency ( $\chi^2=25.33$ ,  $p<0.0001$ ,  $df=4$ , Kruskal-Wallis test; \*  $p<0.05$ , \*\*  $p<0.01$ , \*\*\*  $p<0.001$  for post-hoc pairwise comparisons between individual spatial frequencies). (e, f) With a fine surround texture, both real (e) and simulated (f) saccades were associated with suppression for all spatial frequencies; suppression selectivity<sup>11</sup> was eliminated ( $\chi^2=0.8$ ,  $p=0.938$ ,  $df=4$  for e and  $\chi^2=7.74$ ,  $p=0.102$ ,  $df=4$  for f, Kruskal-Wallis test). Error bars denote s.e.m. across individual subjects’ curves. Supplementary Figs. 8-10 show full time courses as well as controls with black surrounds around the virtual monitor. Note that in d, f, we exploited the longer time course of visual suppression (Fig. 6, Supplementary Figs. 8, 9) to probe perception at a later time than in b, e. This also explains why suppression appeared quantitatively weaker in d, f than in b, e.

1756

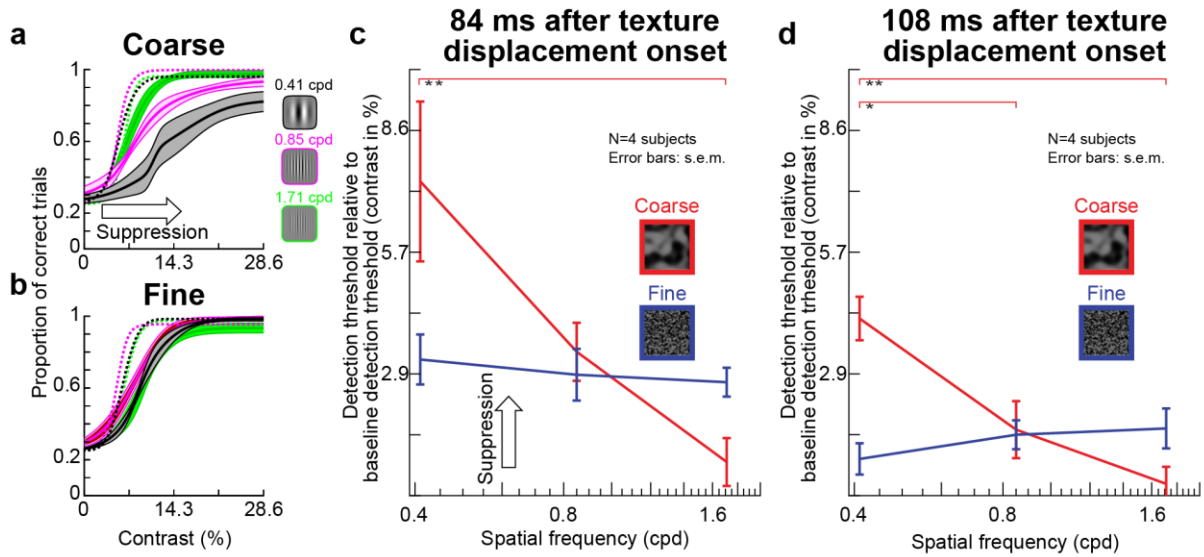


1757  
1758  
1759  
1760  
1761  
1762  
1763  
1764  
1765  
1766  
1767  
1768  
1769  
1770  
1771  
1772  
1773  
1774  
1775  
1776  
1777

**Figure 9 Selective and unselective saccadic suppression measured using full psychometric curves.** (a) We repeated the real saccade experiments of Fig. 8, but with different Gabor grating contrasts (Methods). Different colors indicate different spatial frequencies of the flashed gratings. When the gratings were flashed ~42 ms after saccade onset (Methods) and there was a coarse surround texture, perceptual suppression clearly depended on spatial frequency: detection thresholds were highest for the lowest spatial frequency, and they progressively decreased with increasing spatial frequency. Each curve shows the average of 4 subjects' psychometric curves; error bars denote s.e.m. across subjects. Dashed psychometric curves show perceptual detectability without saccadic suppression (obtained similarly to Fig. 8). (b) When the surround context was fine, rather than coarse, perceptual suppression was not selective for low spatial frequencies (consistent with Fig. 8). (c) Detection thresholds from a, b as a function of grating spatial frequency for flashes ~42 ms after saccade onset. With a coarse surround, detection thresholds were highest for low spatial frequencies and progressively decreased with increasing spatial frequency (1-way ANOVA,  $p=0.0168$ ,  $F=6.6608$ ;  $p=0.0133$  for post-hoc comparison between lowest and highest spatial frequency, indicated by \*). With a fine surround, detection thresholds did not depend on spatial frequency. (d) Same as in c but now for grating flashes occurring ~65 ms after saccade onset. For both surround textures, detection thresholds decreased, indicating perceptual recovery. There was still a trend for dependence of perception on spatial frequency in the coarse condition, consistent with c.

1778

1779



1780

1781

1782

1783

1784

1785

1786

1787

1788

1789

1790

1791

1792

1793

1794

**Figure 10 Selective and unselective saccadic suppression without any saccades.** This figure is identical to Fig. 9, except that real saccades were replaced (in the same subjects) with simulated saccades (exactly as in Fig. 8). All of the same conclusions were reached. There was selective suppression for low spatial frequencies when the texture surround was coarse (**a**); suppression was unselective for grating spatial frequency with a fine surround (**b**); and there was gradual recovery with time (**c**, **d**). In fact, perceptual suppression was clearer and longer lasting in this condition than with real saccades (also consistent with Figs. 1, 6, 8). All other conventions are as in Fig. 9. In **c**, the coarse texture surround showed a significant main effect of spatial frequency (1-way ANOVA,  $p=0.0113$ ,  $F=7.6878$ ;  $p=0.0092$  for post-hoc comparison between lowest and highest spatial frequency, indicated by \*\*). In **d**, the coarse surround also showed a significant main effect of spatial frequency (1-way ANOVA,  $p=0.0019$ ,  $F=13.5276$ ;  $p=0.0017$  for post-hoc comparison between lowest and highest spatial frequency, and  $p=0.0186$  for post-hoc comparison between lowest and intermediate spatial frequency).